



Fluid transport through heterogeneous pore matrices: Multiscale simulation approaches

Cite as: Phys. Fluids **32**, 101301 (2020); <https://doi.org/10.1063/5.0022481>

Submitted: 21 July 2020 . Accepted: 16 September 2020 . Published Online: 09 October 2020

Anh Phan , Dian Fan (范典), and Alberto Striolo 

COLLECTIONS

Paper published as part of the special topic on [Advances in Micro/Nano Fluid Flows: In Memory of Prof. Jason Reese](#)



View Online



Export Citation



CrossMark

ARTICLES YOU MAY BE INTERESTED IN

[Interface learning in fluid dynamics: Statistical inference of closures within micro-macro-coupling models](#)

Phys. Fluids **32**, 091704 (2020); <https://doi.org/10.1063/5.0024670>

[On the wake flow behind a sphere in a pipe flow at low Reynolds numbers](#)

Phys. Fluids **32**, 103605 (2020); <https://doi.org/10.1063/5.0017349>

[Transient magnetohydrodynamic flow and heat transfer of fractional Oldroyd-B fluids in a microchannel with slip boundary condition](#)

Phys. Fluids **32**, 103104 (2020); <https://doi.org/10.1063/5.0025195>

Physics of Fluids
Special Issue on the **Lattice Boltzmann Method**

SUBMIT TODAY!

Fluid transport through heterogeneous pore matrices: Multiscale simulation approaches

Cite as: Phys. Fluids 32, 101301 (2020); doi: 10.1063/5.0022481

Submitted: 21 July 2020 • Accepted: 16 September 2020 •

Published Online: 9 October 2020






View Online



Export Citation



CrossMark

Anh Phan,  Dian Fan (范典),  and Alberto Striolo^{a)} 

AFFILIATIONS

Department of Chemical Engineering, University College London, London WC1E 7JE, United Kingdom

Note: This paper is part of the Special Topic, Advances in Micro-/Nano-fluid Flows: In Memory of Prof. Jason Reese.

^{a)} Author to whom correspondence should be addressed: a.striolo@ucl.ac.uk

ABSTRACT

Fluids confined in nanopores exhibit several unique structural and dynamical characteristics that affect a number of applications in industry as well as natural phenomena. Understanding and predicting the complex fluid behavior under nano-confinement is therefore of key importance, and both experimental and computational approaches have been employed toward this goal. It is now feasible to employ both simulations and theoretical methods, the results of which can be validated by cutting-edge experimental quantification. Nevertheless, predicting fluid transport through heterogeneous pore networks at a scale large enough to be relevant for practical applications remains elusive because one should account for a variety of fluid–rock interactions, a wide range of confined fluid states, as well as pore-edge effects and the existence of preferential pathways, which, together with many other phenomena, affect the results. The aim of this Review is to overview the significance of molecular phenomena on fluid transport in nanoporous media, the capability and shortcomings of both molecular and continuum fluid modeling approaches, and recent progress in multiscale modeling of fluid transport. In our interpretation, a multiscale approach couples a molecular picture for fluid interactions with solid surfaces at the single nanopore level with hierarchical transport analysis through realistic heterogeneous pore networks to balance physical accuracy with computational expense. When possible, comparison against experiments is provided as a guiding roadmap for selecting the appropriate computational methods. The appropriateness of an approach is certainly related to the final application of interest, as different sectors will require different levels of precision in the predictions.

Published under license by AIP Publishing. <https://doi.org/10.1063/5.0022481>

INTRODUCTION

Fluid transport through heterogeneous pore matrices over broadly different time and length scales is at the heart of many technological and environmental processes.^{1–10} Achieving a molecular-level description of fluid–solid interactions and the correlated interfacial dynamics as well as fluid diffusion through heterogeneous pore matrices would help to build quantitative functionality–morphology–transport relationships to enable the manufacture of more efficient and selective porous materials.^{11–16} Molecular simulations can provide molecular structure and dynamics within the interfacial layers, where complex interactions between the porous matrices and fluids occur.^{17–25} Such simulations, however, tend to be limited to single nano- to meso-pores of simple geometry, which falls short of accounting for the porous material complexity at larger length scales. On the other hand, approaches accounting for the latter must rely on a simplified picture of the confined fluid and

its transport properties.^{26–28} Achieving a balance between the two approaches remains a challenge, especially because different applications require different levels of precision in the predictions, while in most cases, it is preferable to obtain results at low to moderate computational costs.

In what follows, we present the selected simulation results to highlight the significant impact of the fluid structure on its dynamical behavior in a single pore at the nanoscale and compare them against experimental data at various length scales to assess the reliability of various approaches, when possible. Convective motion and molecular diffusion are the two main mechanisms responsible for fluid dynamics in porous matrices. Molecular diffusion becomes the dominant mechanism when fluids are confined in pores of size comparable to the size of the confined fluid molecules (i.e., in nanopores). The geometry of the nano-/meso-pores and their pore apertures as well as pore connectivity play an important role in regulating the amount of fluids that cross or enter natural porous

media.^{29–31} Because many pores in the subsurface are in this size regime,⁸ it is crucial to understand the mechanisms by which the molecular diffusion occurs in nanopores, and when surfaces and pore defects strongly affect the transport mechanisms. To illustrate these concepts, we summarize the selected studies for fluid transport in slit-shaped single nanopores primarily from our body of work, produced by employing atomistic molecular dynamics (MD) simulations. It should be recognized that many groups contributed to these investigations. The interested reader is referred to a few recent reviews on this topic.^{18,32–34}

Bridging the gaps between the results obtained within a single pore, a few pores, a few hundreds of pores, and ultimately within complex pore networks requires the development of simulation approaches with high computational efficiency. In principle, atomistic MD is able to describe molecular phenomena even when they occur in large systems. However, it requires high computational resources, and therefore, it can become inefficient and sometimes impractical to study fluid transport through heterogeneous porous matrices at length and time scales larger than a few nm and several hundreds of ns, respectively.³⁵ When practical applications require modeling such conditions, continuum fluid models, such as the no-slip Hagen–Poiseuille flow equation or Darcy's law, are often employed, although they do not correctly characterize flow within complex nanoporous materials because in such systems, non-continuum flow phenomena arise due to the well-ordered molecular structure near solid–liquid interfaces, inaccurate characterization of the local viscosity, and interfacial slip.³⁵ In Fig. 1, we

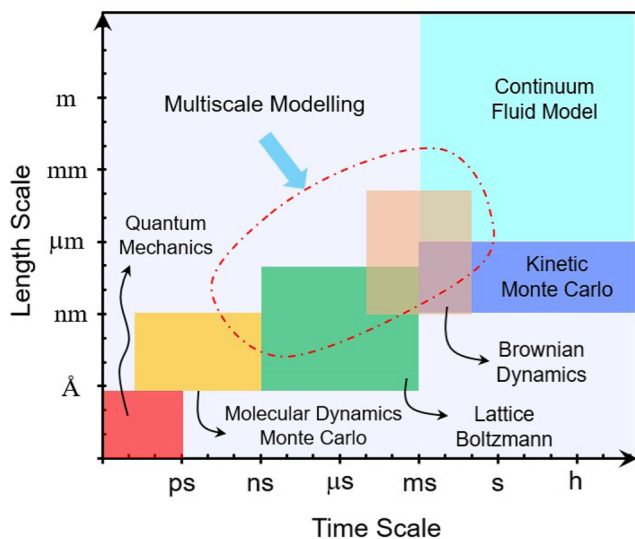


FIG. 1. Time and length scales in which atomistic MD simulations, lattice Boltzmann, kinetic Monte Carlo, macroscopic continuum fluid model, and multiple modeling approaches are used. The approach identified as “multiscale” seeks to reconcile the results from the different methods toward describing fluid transport both precisely (e.g., taking into consideration molecular phenomena) and effectively (e.g., achieving length scales relevant for the applications). Reproduced with permission from Vlachos, “A review of multiscale Analysis: Examples from systems biology, materials engineering, and other fluid–surface interacting systems,” *Adv. Chem. Eng.* **30**, 1–61 (2004).³⁶ Copyright 2005 Elsevier B.V.

summarize time and length scales in which atomistic MD simulations as well as Monte Carlo, lattice Boltzmann (LB), Kinetic Monte Carlo (KMC), macroscopic continuum fluid model, and multiple modeling approaches are typically used. Developing a computational framework to couple all these techniques remains challenging but promises the ability to capture phenomena that occur at the single-pore level (e.g., edge effects) with larger-scale phenomena (e.g., preferential flow pathways) toward truly predicting fluid transport through heterogeneous porous matrices. Note that in the shortest time and length scales, one could implement quantum mechanics methods to elucidate interactions between fluids and pore surfaces, which could lead to reactivity.

We review in what follows some promising advances for the development and implementation of multi-scale approaches achieved by implementing non-equilibrium MD simulations, coupling MD simulations with LB calculations, stochastic approaches based on KMC, and improved continuum macroscopic flow models. We attempt to identify conditions under which each multiscale approach is preferable, based on comparison against the available experimental studies. The experimental tools considered include pulsed field gradient nuclear magnetic resonance (NMR),^{37–39} quasi-elastic neutron scattering (QENS),^{38–40} and microimaging,^{41–43} among others.

The remainder of this Review is organized as follows: In the section titled Fluid transport in single nanopores, we present the selected MD results for the fluid structure and transport behavior in single nanopores and discuss the inaccuracy of the conventional continuum fluid model owing to the dominance of non-continuum flow phenomena. Then, in the section titled Fluid transport in hierarchical pores, we present some multiscale approaches that address the aforementioned challenges. We conclude presenting open questions and some emerging topics we consider promising testbeds for future research.

FLUID TRANSPORT IN SINGLE NANOPORES

Fluid structure governs diffusion enhancement/hindrance

Mounting evidence, albeit mostly from computational studies, suggests that confinement significantly affects almost all the fluid properties related to interfacial interactions (adsorption and solubility), thermophysical (phase behavior), dynamical (translational, rotational, and vibrational diffusions), and ultimately transport properties of the confined species.^{8,47} Because understanding the structural and dynamical properties of fluid species such as carbon dioxide (CO₂) and methane (CH₄) confined in nano- and mesopores in sedimentary rocks is of increasing interest, MD simulations at reservoir composition^{48,49} have been used by Loganathan *et al.*⁴⁴ to quantify the partitioning of CO₂ and methane between bulk and nano- and meso-pores bounded by the montmorillonite clay mineral. MD has been proven useful to study multi-component systems described at the atomistic level. In MD, interactions between atoms and molecules are described explicitly via appropriate atomic force fields. The motion of such entities is described by solving numerically Newton's equations of motion. The resultant molecular trajectories, integrated over time, yield the macroscopic properties of such systems via statistical mechanics analysis.⁵⁰ For example, in Fig. 2(a)

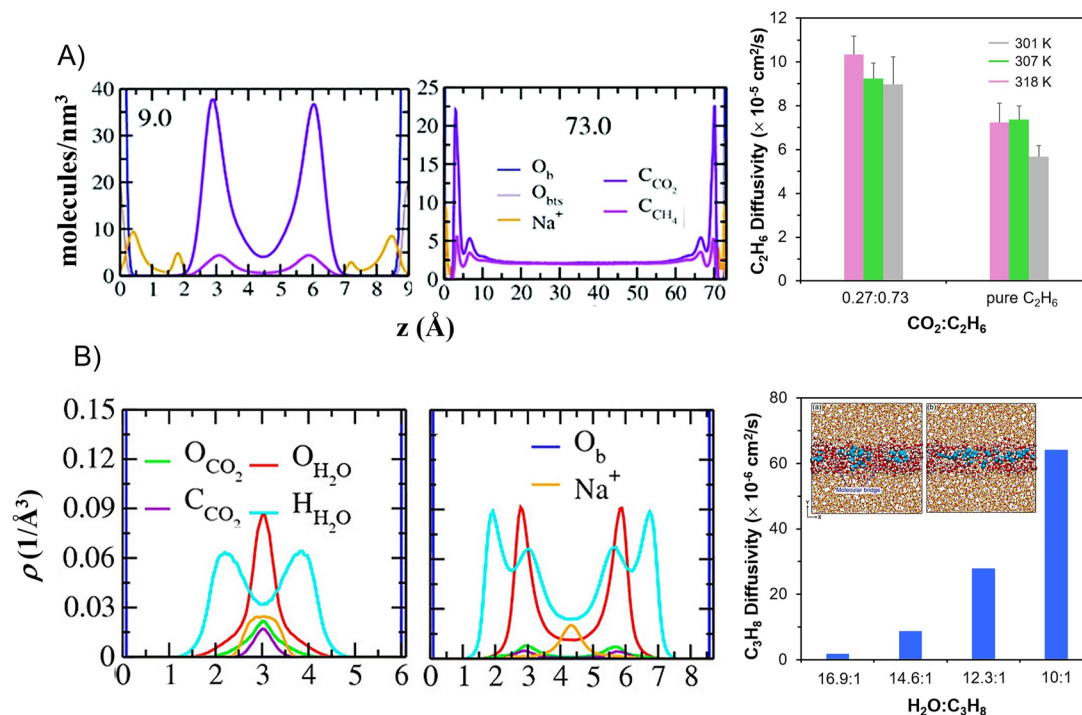


FIG. 2. (a) Left: density profiles of Na^+ (orange), C_{CO_2} (violet), and C_{CH_4} (magenta) as a function of the distance z across the clay nano- (middle) and meso-pore (bottom). Reproduced with permission from Loganathan *et al.*, "Understanding methane/carbon dioxide partitioning in clay nano- and meso-pores with constant reservoir composition molecular dynamics modeling," *Phys. Chem. Chem. Phys.* **21**(13), 6917–6924 (2019). Copyright 2019 PCCP Owner Societies. Right: self-diffusion coefficients estimated for C_2H_6 in the presence of CO_2 in silica pores from QENS experiments. Figures adapted with permission from Patankar *et al.*, "Role of confinement on adsorption and dynamics of ethane and an ethane– CO_2 mixture in mesoporous CPG silica," *J. Phys. Chem. C* **120**(9), 4843–4853 (2016). Copyright 2016 American Chemical Society. (b) Left: atomic density profiles of O_b (dark blue vertical), Na^+ (orange), $\text{O}_{\text{H}_2\text{O}}$ (red), $\text{H}_{\text{H}_2\text{O}}$ (cyan), O_{CO_2} (green), and C_{CO_2} (violet) as a function of the distance z across the smectite clay pores with the monolayer (left) and bilayer (right) hydration basal spacing at 348 K and 90 bars. Right: 1D self-diffusion coefficients estimated for propane confined in silica pores at different water loadings. Figures adapted with permission from Loganathan *et al.*, "Molecular dynamics study of CO_2 and H_2O intercalation in smectite clays: Effect of temperature and pressure on interlayer structure and dynamics in hectorite," *J. Phys. Chem. C* **121**(44), 24527 (2017) and Le *et al.*, "Propane-water mixtures confined within cylindrical silica nanopores: Structural and dynamical properties probed by molecular dynamics," *Langmuir* **33**(42), 11310 (2017). Copyright 2017 American Chemical Society.

(left), the results show the preferential adsorption of CO_2 on clay surfaces, suggesting that CO_2 can effectively remove methane from such pores, leading to enhanced oil recovery and shale gas production. It is worth pointing out that the accumulation of fluids near pore surfaces leads to more frequent fluid–fluid and fluid–pore collisions, which reduce the mean free path (MFP) and the diffusion coefficient, and that this effect is more and more pronounced as the pores become narrower and narrower, e.g., micro-pores. By employing the Direct Simulation Monte Carlo (DSMC) method and MD simulations, Xie and his co-workers⁵¹ showed that the MFP is spatially dependent when both the intermolecular interactions between gas molecules and collisions between gas molecules and wall atoms are taken into consideration. The behavior of fluid confined within larger meso-pores, on the other hand, may exhibit fluid–substrate interfacial and bulk-like properties simultaneously, with the latter becoming dominant as the pore width increases.⁴⁵ To support simulation results such as those in Fig. 2, one could employ QENS. For example, conducting QENS for ethane in mesoporous silica pores, Patankar *et al.* found that the self-diffusion coefficient of ethane confined in 11.1 nm and 41.5 nm pores was ~ 4 times slower than

that observed in the bulk under otherwise similar conditions.⁴⁵ If these results are due to the enhanced fluid density near the pore walls, it might be feasible to facilitate the fluid diffusion by adding a second fluid that preferentially adsorbs on the solid substrate, as discussed previously. Indeed, one QENS experimental study⁴⁵ reported that the ethane diffusion in mesoporous silica increased in the presence of CO_2 (27 mol. % CO_2) by a factor of ~ 2 compared to the data obtained for pure ethane [see Fig. 2(a), right]. Le *et al.*²³ conducted MD simulations for systems containing butane and CO_2 in a ~ 2 nm wide slit-shaped silica pore. The results also showed that CO_2 preferentially adsorbed near the pore surfaces, consistent with the results reported in Fig. 2(a) (left),⁴⁴ enhanced diffusion of butane occupied in the middle of the pore, via a "molecular lubrication" mechanism, which is in good agreement with the prior experimental study.²³ Others also observed that CO_2 enhanced the diffusion of hydrocarbons through different porous materials.^{52–54}

The preferential adsorption of CO_2 to the pore surfaces can enhance hydrocarbon diffusion in nanopores, but one can question whether it is possible to achieve similar results if another fluid other than CO_2 , also preferentially attracted or even more strongly

adsorbed to the pore surface, is used. Recently, Loganathan *et al.*⁴⁶ employed Grand Canonical MD (GCMD) simulations to investigate the structure and dynamics of CO₂–water mixtures in the interlayers of the smectite clay, Na-hectorite, at geological temperatures and pressures. The GCMD algorithm is a hybrid MD-Monte Carlo technique, which was introduced to maintain constant temperature and chemical potential during the virtual experiment. The approach assures that the number of particles and system energy varies corresponding to the standard grand canonical probability distribution.⁵⁵ In the GCMD approach, it is possible to use the grand canonical Monte Carlo algorithm to first establish and subsequently maintain a chemical potential gradient across a pore, while MD allows one to study the transport of fluids across the pore in response to the chemical potential gradient. Details of the GCMD simulations can be found in the work of Boinepalli and Attard.⁵⁵ In Fig. 2(b) (left), Loganathan *et al.* showed that water is more strongly adsorbed on the clay surfaces than CO₂, displacing CO₂ to the midplane of clay interlayers for the monolayer hydration structure (left) and closer to one of the basal surfaces for the bilayer hydration structure (right). Coming back to the question whether diffusion enhancement is observed if another fluid other than CO₂, e.g., water, is mixed with hydrocarbon, Gautam *et al.*⁵⁶ used QENS experiments to examine the diffusion of propane in silica-based, cylindrical pores of diameter ~ 1.5 nm in the presence of water. The experimental results showed that water hampered, rather than facilitated, propane diffusion. To provide a molecular understanding of these observations, Le *et al.*²⁵ conducted MD simulations for a system resembling the experimental one.⁵⁶ The results showed that although water molecules are strongly adsorbed on the pore surface due to such a narrow pore diameter as well as to the strong water–water interactions, water molecules can form molecular bridges across the pore volume, which impedes propane diffusion. Le *et al.*²⁵ quantitatively examined the decrease in propane diffusion upon the increase in water loading inside the pore [as shown in Fig. 2(b), right].

The approaches implemented to conduct these investigations could be relevant for studying systems with extremely heterogeneous pores of size comparable to that of the fluid molecules. When the two or more fluids confined in a narrow pore are mixable, however, the phenomena of interest could be different compared to those discussed so far, and the diffusion of a fluid dissolved within another fluid, the latter confined in a pore, needs to be investigated.

Confined fluids regulate diffusion

The transport behavior of guest molecules inside narrow pores in the presence of confined fluids is strongly dependent on the chemical properties of mineral solid substrates, as well as on the chemical nature of the fluid molecules in question. Bui *et al.*¹⁹ reported that the self-diffusion coefficients estimated for methane confined in water-filled pores carved out of common minerals can vary by a factor of ~ 4 , although the simulations were conducted under the same conditions (i.e., of the same pore width and temperature). Very few experimental studies on the properties of methane in confined water within nanopores have been conducted. However, Hu *et al.*⁵⁷ recently employed NMR to study the behavior of water and methane within ZSM-22, MCM-41, and SBA-15 nanopores. These materials contain mostly the two most common elements on the

Earth (O and Si) and possess uniform one-dimensional pore sizes of ~ 0.5 nm, 3 nm, and 6 nm, respectively, which enables the quantification of pore size effects on transport. Hu *et al.* found that the self-diffusion coefficients of methane in water-filled ZSM-22 pores with pore sizes of ~ 0.5 nm have a similar order of magnitude to those found in our previous simulation²¹ ($\sim 10^{-10}$ m²/s). Additional insights into multicomponent interactions under nanoconfinement were recently achieved by simulations.^{58–60} For example, Ho *et al.*⁵⁸ showed that a thin supercritical CO₂ layer formed at water–solid interfaces could help accelerate water flow through a rough hydrophilic nanochannel, acting as a molecular lubricant that converts a stick-to-slip flow in nanopores.

While equilibrium MD simulations can be used to quantify the structure of confined fluids and their diffusion properties, non-equilibrium MD (NEMD) can be implemented to assess the transport properties of fluids confined in narrow pores, although usually in single pores because of the computational requirements.^{61–64} In NEMD algorithms, the equations of motion are integrated numerically as is the case of equilibrium MD, but an external field is applied to impose, for example, a pressure gradient across a pore. More details have been described in some previous works.^{61,65,66} Considering as an example the recent results from our group, Phan *et al.*²¹ studied the transport properties of a gas mixture [ethane, methane, and hydrogen sulfide (H₂S)] through hydrated nanopores. The results showed that H₂S could permeate the hydrated pores much faster than the other species and that ethane is too large to transverse effectively the water-filled nanopores. This could have significant implications in several applications, such as the design of gas separation membranes and the shale gas sustainable deployment.

One might ask whether a similar transport behavior in narrow pores would be achieved when a fluid other than water, also strongly adsorbed on the pore surface, was present. One such fluid could be benzene, which could be a first approximation for aromatic hydrocarbons trapped in sedimentary rocks. Employing the boundary-driven NEMD (BD-NEMD) algorithm,⁶¹ Phan *et al.*⁶⁷ studied the transport properties of two fluid mixtures (CO₂–methane and H₂S–methane) through amorphous silica nanopores filled with benzene. The BD-NEMD simulations are implemented by applying a constant force along the x axis, acting in the direction of the arrows (see Fig. 3, top) to all CO₂, H₂S, and methane molecules located in a thin slab (shaded region) of width $d_{ext} = 20$ Å within the permeate region of the simulation box. This external field establishes and maintains a constant pressure difference across the pore network and hence leads to a steady molar flux across the hierarchical porous media. For mixtures, the transport diffusivity of each component is estimated by dividing its permeability, estimated based on the linear relationship between the permeated number of molecules and time, by its solubility within the pore. The system considered in Fig. 3 was built as an approximate representation of organic-rich shale caprocks that contain a significant amount of organic carbon (>11.7 wt. %). Snapshots representing the simulated systems are shown in Fig. 3 (top).⁶⁸ Analysis of the simulation results shows that both CO₂ and H₂S are favorably adsorbed inside the organic-filled pore, in part, displacing benzene. Surprisingly, CO₂/H₂S adsorption facilitates methane transport, as illustrated in Fig. 3 (bottom), because both fluids play a role as mobile carriers and possibly trigger benzene swelling, creating favored traveling paths within the

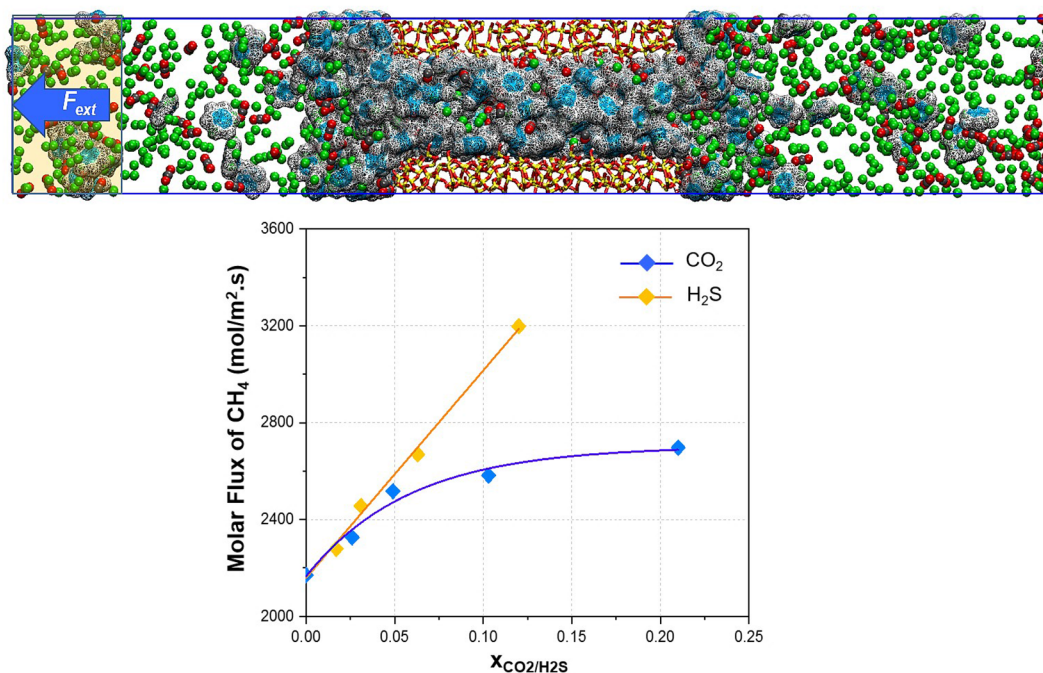


FIG. 3. Top: representative simulation snapshots for a filled pore exposed to the bulk reservoirs along the x direction. The amorphous silica nanopore is filled with 400 benzene molecules, providing a model for oil trapped in sedimentary rocks. Bottom: molar flux of methane in CO_2 - CH_4 (blue) and H_2S - CH_4 (yellow) mixtures across the benzene-filled silica nanopore as a function of CO_2/H_2S bulk mole fraction. Figures adapted with permission from Phan and Striolo, “Evidence of facilitated transport in crowded nanopores,” *J. Phys. Chem. Lett.* **11**(5), 1814–1821 (2020). Copyright 2020 American Chemical Society.

pore networks.⁶⁷ Results such as those just summarized could help to determine unanticipated transport mechanisms and building up engineering approaches for CO_2 capture and storage in caprocks, albeit their effect on macroscopic transport needs to be quantified.

Related to shale gas, it remains of great interest to quantify how hydrocarbons can be produced from the source rocks. Indeed, many investigated how hydrocarbons escape from kerogen.^{2–4,8,18}

Breakdown of continuum fluid models at the nanoscale

Falk *et al.* employed MD to calculate hydrocarbon transport in kerogen [see Fig. 4(a)] and statistical mechanics to analyze the results.⁶⁹ They reported that the continuum Darcy’s law, derived from the Navier–Stokes equation,⁷⁰ a fundamental principle for computational fluid dynamics (CFD) studies, fails to predict hydrocarbon permeability in shale nanoporous matrices—i.e., the kerogen material. In particular, the permeability k ($k = K \times \eta$ with permeance K and viscosity η), an elemental material characteristic, was observed to depend not only on the adsorbed amount but also on the fluid type [see Fig. 4(b)].⁶⁹ The failure of the continuum flow description is likely due to adsorption. Because of the drastic confinement in the nanopores present in kerogen, the physical state of confined alkanes is remarkably different from their bulk counterpart at the same temperature and pressure, changing from the gaseous phase in the bulk to a condensed liquid-like phase under confinement. These results demonstrate that calculating flow properties in

the nanopores using bulk viscosity can lead to inappropriate conclusions. Falk *et al.*⁶⁹ showed that also using the viscosities correspondent to the confined alkane density would not yield permeability predictions, using Darcy’s law, in agreement with the MD simulation results [see the inset of Fig. 4(b)].

To alleviate the shortcomings of Darcy’s approach, many corrections have been suggested, for example, by invoking slippage in gas flow via the Klinkenberg effect.⁶⁹ Some have attempted to use MD data to correct the Hagen–Poiseuille (H–P) flow equation, introducing a Navier slip boundary condition (BC) for simulating flows in nanotubes with size of a few nm.⁷¹ For example, Walther *et al.*⁷² modified the H–P equation with the pressure correction proposed by Weissberg⁷³ to take into consideration the membrane-end losses. Nevertheless, these empirical corrections cannot completely account for the entirety of the complex behavior of hydrocarbons in heterogeneous nano-porous materials.

Atomistic MD is probably the most appropriate approach for accounting for non-continuum flow inside nano-porous materials.^{2–4,8,18} However, this technique requires enormous computational resources when it is desired to study flow through pores longer and wider than a few tens of nanometers.⁷⁴ On the other hand, non-continuum effects ranging from molecular ordering to velocity slip can inhibit the reliability of continuum fluid models such as CFD.⁷⁴ Is it possible to achieve more reliable and computationally efficient predictions toward gas transport in heterogeneous pore networks at a larger scale? The challenge lies in upscaling the simulation results

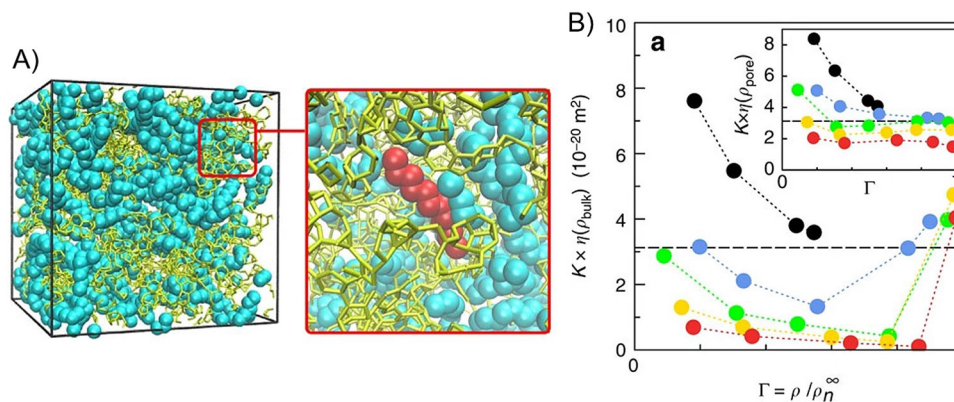


FIG. 4. (a) Hydrocarbons adsorbed in kerogen-like nanoporous carbon and zoom on one dodecane molecule (red) with its neighbors and the surrounding carbon structure. (b) Permeability vs loading, showing the breakdown of the hydrodynamic prediction for the permeance: methane (black), propane (blue), hexane (green), nonane (yellow), and dodecane (red). The viscosity is that of the bulk hydrocarbon at the corresponding pressure and temperature. For comparison, the dashed lines give the permeability of a cylindrical pore with diameter equal to the mean size of the matrix pore-size distribution. Figures adapted with permission from Falk *et al.*, “Subcontinuum mass transport of condensed hydrocarbons in nanoporous media,” *Nat. Commun.* **6**, 6949 (2015). Copyright 2015 Springer Nature.

achieved in a single pore, toward predicting flow transport through a pore matrix, as different phenomena involved in such multiscale porous matrices can affect the results.

FLUID TRANSPORT IN HIERARCHICAL PORES

Brute force non-equilibrium MD simulations with predictive empirical relations

Fluid transport through heterogeneous pore networks is usually characterized through the tortuosity parameter τ (resistivity to transport).^{75,76} This parameter relates the flux J to porosity ϕ and flux in the absence of medium J_0 through the following expression: $J = \phi/\tau J_0$. While porosity ϕ is estimated using adsorption experiments, permeability/transport and NMR experiments can be used to measure both J and J_0 (and, therefore, extract τ).¹⁸ From a numerical perspective, tortuosity can be assessed from x-ray tomography experiments⁷⁷ using, for example, random-walk (Brownian motion) simulations where the tortuosity is estimated as the square ratio between the walking path length and the length along the longitudinal coordinate.

To replicate such experiments via a direct atomistic simulation approach, Phan *et al.*¹⁷ employed the BD-NEMD algorithm⁶¹ (as mentioned above) to examine methane flow through hierarchical amorphous silica porous materials. Note that for single component systems, e.g., only methane through porous media, transport diffusivity can be estimated from the pressure gradient and molar flux, which were quantified by fitting the steady-state simulation results to Fick’s first law. The pore networks considered in Fig. 5 were meant to represent the simplified structure for some of those often found in shale formations. By conducting simulations on “synthetic” model porous media, the transport properties (e.g., permeability and diffusivity) are collected and correlated with pore structure information. In Fig. 5(a), the results show a strong dependence of the methane permeability through the pores on the frameworks. Indeed, a linear

correlation was observed between methane permeability and a characteristic parameter that accounts for porosity, constriction factor, and tortuosity [see Fig. 5(b)]. The constriction factor, a geometric parameter that can become important when the fluid molecules have size comparable to the pore size, was calculated as a function of cross-sectional area $A(x)$ of a porous medium along the direction of transport and its length L . The simulation results suggest that the correlation identified by Phan *et al.* applies for hierarchical porous materials consisting of both micropores and mesopores. Ultimately, Phan *et al.* found that the transport properties of methane through porous media scale as a power-law function of porosity and constriction factor [as shown in Fig. 5(c), left], which are descriptors that can be determined experimentally. Phan *et al.* identified as exceptions those porous systems that containing extremely strong blockages [system 3 (green) or 8 (orange)]. These results suggest that when characterization data are accessible, it is possible to forecast transport properties for engineering and natural materials. For example, a power law is also obtained for Fontainebleau sandstone [see Fig. 5(c), right].^{78,79} The good agreement proposes that the method employed is capable of quantifying molecular effects on fluid transport as well as reliably predicting fluid transport properties through shale rocks using macroscopic pore characterization data as a sole input.

While important new insights can be achieved from the above method, modeling and upscaling approaches for describing fluid transport within realistic and more complex porous materials are still missing, as NEMD cannot be implemented for systems much larger than those considered in Fig. 5. To overcome the computational barriers, numerous computational and theoretical approaches have been attempted, including coarse-grained MD simulations,^{80,81} LB calculations,^{82–84} stochastic KMC algorithms,^{85–87} random-walk particle-tracking (RWPT) method, and modified macroscopic continuum flow model. Each method displays advantages and suffers from limitations, relying upon the simulation time scale and the size of the samples considered. The goal remains to access further

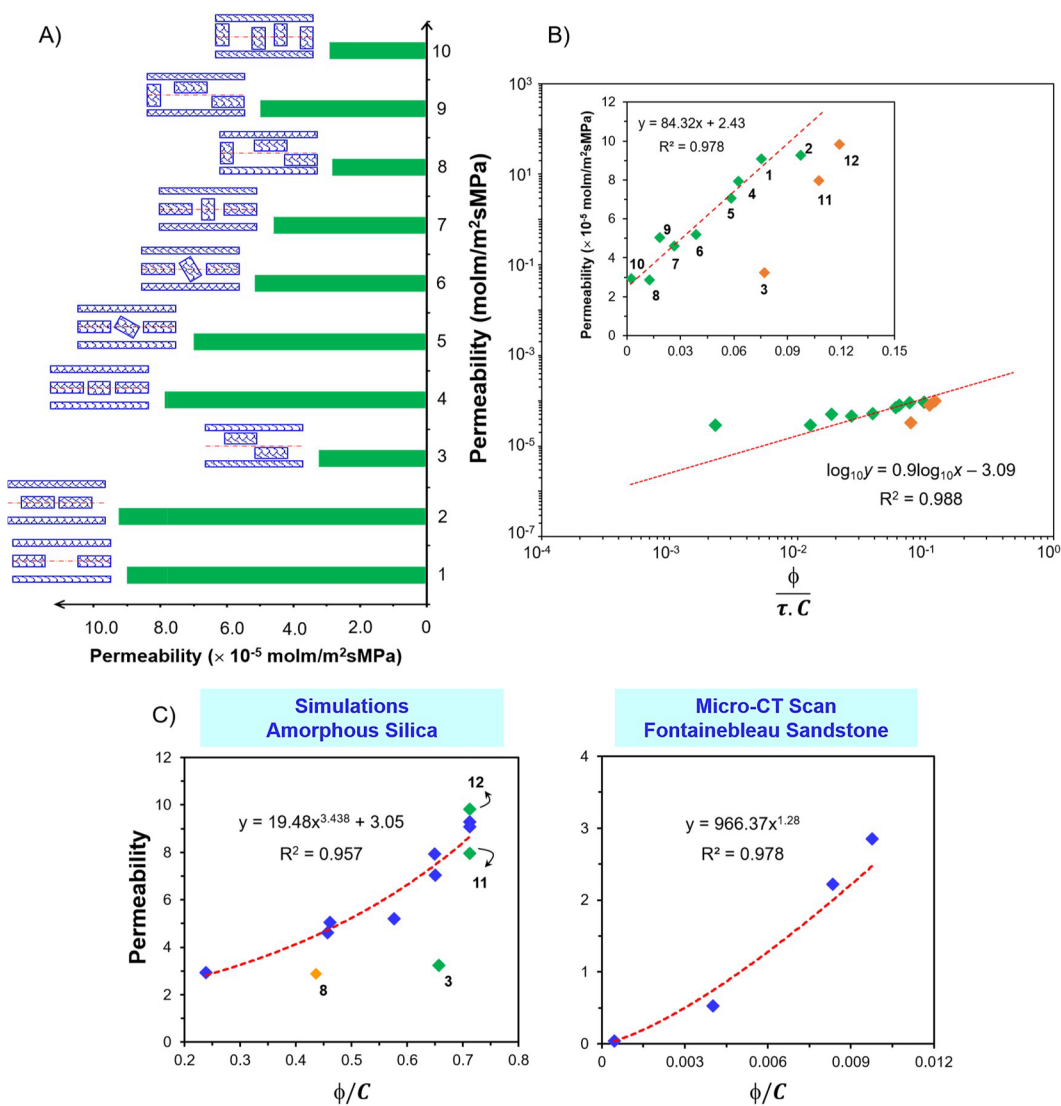


FIG. 5. (a) Permeability as determined by BD-NEMD simulations for methane across the ten porous model systems. (b) Methane permeability as a function of the pore characteristic parameter defined by the ratio of porosity to tortuosity and constriction factor on logarithmic plots. The insets provide representations for the data on Cartesian plots. Results were obtained for all hierarchical pore model systems. (c) Correlation between permeability and the ratio of porosity to constriction factor. The results from the simulations for hierarchical amorphous silica porous materials in this study,¹⁷ and those from micro-CT scan and experiments for the Fontainebleau sandstone are shown in left and right panels, respectively. Figures adapted with permission from Phan and Striolo, "Methane transport through hierarchical silica microporous materials: From non-equilibrium atomistic simulations to phenomenological correlations," *Microporous Mesoporous Mater.* **288**, 109559 (2019). Copyright 2019 Elsevier B.V.

length and longer time scales while realistically accounting for hierarchically complex porous materials, fluid–rock interactions, and the wide range of confined fluid states.

Coupling MD and LB simulations

As already mentioned, in principle, MD simulations could describe microscopic transport phenomena accurately, but their applicability to large length scales (e.g., >100 nm) is drastically

restricted by the availability of computing resources.^{88,89} As an alternative, since the 1980s, the LB method has become attractive to overcome the computational limitations that MD simulations entail.⁹⁰ Compared to MD simulations, the virtue of the LB method is its capability of mesoscale characterization of fluid transport and fluid–solid interactions in porous media with complex boundary geometries, which renders it a computationally affordable and reasonably accurate alternative to model microscopic transport.^{91–93} The LB method considers fluid flow as a collection of hypothetical

particles described by appropriate particle velocity distribution functions. These particles, located on the lattice fluid nodes, exchange and propagate velocity distribution values after their collision with other particles, as well as with the walls, which are represented as solid nodes.⁹⁴ A typical LB implementation for microflow requires the input of initial fluid density and momentum and the prescription of BCs (e.g., fluid–solid interface and periodic boundaries), which can be obtained from the correspondent MD models.⁸⁴

During the past few decades, the LB approach has been extensively developed and applied to study flow in confinement,^{95–99} from transport through T-/Y-junctions,¹⁰⁰ near nanotubes,¹⁰¹ corrugated surfaces,^{102,103} nano-/micro-channels,^{95,104–106} and nano-/micro-porous complex media.^{107–109} Of interest for the present overview is (1) how accurate the LB results can be at the microscale, e.g., compared to their counterpart MD models, and (2) how MD data can be mapped into LB implementations to improve the LB predictions. In fact, MD simulation results are often used to benchmark and identify the applicability range of LB models:^{95,110–113} Myriad studies have shown that LB algorithms are capable of reproducing MD results, except at the nano-scale interfaces¹¹⁴ or under conditions of extreme confinement.¹¹⁵ These findings provide best practice approaches to couple MD onto LB to yield reliable predictions.

Numerous coupling approaches have been developed to further improve the LB accuracy.^{96,116,117} One such approach is the two-way coupling of data (e.g., velocity) exchange at the overlapping regions of the MD and LB domains during the simulation, which applies to fluid–substrate interactions for confined single-phase transport as well as to fluid–fluid interactions for multiphase transport.^{96,101} This coupling usually applies to the cases where nano-scale simulations are needed regionally only, such as for the description of fluid transport around a nanotube¹⁰¹ (where LB and MD are applied to the continuum domain and around the nanotube, respectively) or that of fluid transport through a nanochannel¹¹⁸ (where the bulk region inside the nanochannel is described by the LB method, while the interfacial phenomena, such as fluid slip, are described by MD simulations).

The key to the success of this approach is the agreement between LB and MD results in the overlapping domain or at the interfacial BC between the two subdomains. An example data-exchange protocol is the one in which the molecule velocity at the interface in the MD model is reset to match a given distribution (e.g., Maxwellian) with mean and variance dictated by the LB results; in contrast, the particle velocity distribution in the LB model is reconstructed to match the homogenized MD results near the interface.⁹⁶ While this approach is very promising, its computational efficiency is limited by the need of securing convergence between MD and LB methods in the interfacial region.

An alternative coupling approach, which is less computationally demanding because it does not require synchronization between MD and LB datasets, is the “one-way mapping” of the final MD results into the implementations of larger-scale LB models. Successful examples involve the mapping of slip length,^{119,120} fluid viscosity,¹¹⁹ interfacial tension,^{121,122} adsorption layers,¹²³ and velocity profiles⁸⁴ as obtained from MD simulations into the correspondent LB models. An exemplar of the latter approach is the use of MD velocity data to identify suitable BCs to be implemented in the correspondent LB models.^{84,124,125} In this approach, velocity data

from MD simulations are often normalized by the bulk velocity.^{107,126,127} Once the normalized LB velocity results match the correspondent MD data, the LB model is regarded as valid and representative of the physics at the solid–gas interface. However, recent results^{84,128} suggest that this approach may not be always accurate when using MD or DSMC data. For example, one study¹²⁸ showed that two LB models, which implemented (1) the combined scheme of diffuse reflection and bounced-back BCs and (2) discrete Maxwellian BCs, respectively, successfully predicted the normalized velocity from the DSMC; however, only the former scheme reproduced the dimensionless flux, while the latter overestimated the dimensionless flux in transition flow regimes.

Similar observations were achieved in a comparative LB vs MD study from our group.⁸⁴ As shown in Fig. 6(a), four LB models implementing different BCs (denoted as BC1–4, details of BCs are referred to as in the caption of Fig. 6) predict *similarly* agreeable velocity profiles when compared to MD data; however, not all LB models accurately predict the gas permeability correction factor as observed from core-flooding experiments [see Fig. 6(e): overestimation by implementing BC1 and BC3], which implies that the normalized velocity in Fig. 6(a) may not be the proper method to identify correct BCs for the LB calculations.⁸⁴ It was instead suggested that using the non-normalized axial velocity¹¹³ data from the correspondent MD models [Fig. 6(b)] can identify the correct BCs [i.e., see the good agreement of velocity predictions from the MD and LB results by implementing BC4 in Figs. 6(b)–6(d)]. It was shown that by implementing the newly identified BCs in the LB calculations, it is possible to reproduce the permeability correction factor measured experimentally [see Fig. 6(e)].

Slip boundary conditions in LB simulations

As indicated in Fig. 6, the choice of the BC strongly impacts the LB predictions for properties such as permeability.^{135–137} When using MD data to benchmark LB models, it is, therefore, crucial to understand the applicability of different slip boundaries in the LB method. MD has been used to identify slip BCs in a variety of conditions, sometimes achieving the unexpected results.¹³⁸

In LB calculations, the shape of the boundary segments embedded in each lattice site is considered either planar or curved (non-planar), reflecting the physical structure of porous media. The physical boundary is often approximated as zigzag segments, i.e., the planar boundary. The drawback of this approximation is that it decreases the resolution of images while depicting porous media, and therefore, it can impact the accuracy of LB results; on the other hand, if the image is converted into high-resolution pixelated planar boundaries, the computational time of the subsequent LB simulations can be long, as well as the efforts required to build the model for the LB calculations themselves. The choice of specific BCs for describing gas slip over planar surfaces has been extensively reviewed in the literature,^{94,99,130,139} including diffuse reflection,^{140,141} specular reflection,¹⁴² the combined bounce-back and specular reflection,¹⁴³ and the combined diffuse reflection and specular reflection.¹⁴⁴ In contrast to planar boundaries, the curved boundaries can better maintain the physical structure of the porous media and can overcome the resolution limitations imposed by

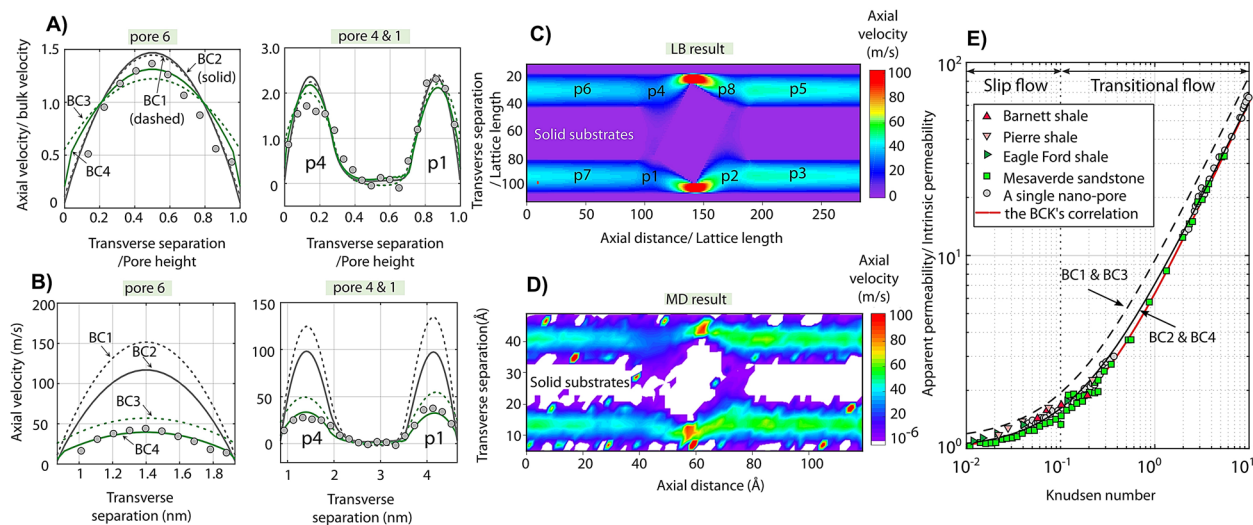


FIG. 6. Use of MD velocity data to identify suitable BCs for LB simulations.⁸⁴ (a) Normalized axial velocity by the bulk velocity. (b) Axial velocity. Legends: MD results (dots), LB results (lines): BC1 (classical bounce-back scheme), BC2 (improved bounce-back scheme), BC3 (the combined scheme of the classical bounce-back and specular reflection), and BC4 (the combined scheme of the improved bounce-back and specular reflection). Compared to BC1, BC2 imposes an extra constraint on the velocity vectors parallel to the fluid–solid interface (details of the algorithm are referred to Refs. 84 and 129). Axial velocity distribution obtained from (c) LB (by implementing BC4) and (d) MD simulations of gas flow through a porous medium where p1–p8 denote connected pores. (e) Estimation of the permeability correction factor, i.e., the ratio of apparent permeability to intrinsic permeability of the porous medium of the structure in (c). The results represented by the black dashed line are obtained by implementing BC1 for intrinsic permeability and BC3 for apparent permeability. The results represented by the black solid line are obtained by implementing BC2 for intrinsic permeability and BC4 for apparent permeability. Also presented are core-flooding measurement in nanoporous samples^{130–132} and the Beskok–Karniadakis–Civan’s (BKC) correlation^{133,134} reported in the literature. Figures adapted with permission from Fan *et al.*, “Accurate permeability prediction in tight gas rocks via lattice Boltzmann simulations with an improved boundary condition,” *J. Nat. Gas Sci. Eng.* **73**, 103049 (2020). Copyright 2020 Elsevier B.V.

the planar approximation. However, accounting for the slip over curved, and in general, non-planar boundaries has been a challenging task at the LB level.^{145,146} The common solution is to interpolate the local velocity distribution functions according to the relative distance between fluid node, solid node, and wall.^{125,147–149} The relationships between the incoming and outgoing velocity distribution functions are then stipulated by the specific slip BCs, e.g., the interpolated bounce-back,¹⁴⁷ interpolated combined bounce-back and diffuse reflection,¹²⁵ interpolated combined bounce-back and Maxwellian diffuse reflection,^{145,148} and multi-reflection scheme,¹⁴⁹ which are adapted from planar BCs. Alternative solutions to describe slip on curved boundaries may resort to changing the coordinate system, e.g., to adopt a body fitted curvilinear coordinate system when using the combined bounce-back and specular reflection scheme,¹⁵⁰ or to reconstruct velocity BCs, e.g., using Navier’s slip length to derive the velocity at the wall,¹⁵¹ or adopting a method that counter-extrapolates slip velocity and non-equilibrium velocity distribution function.¹⁵²

Using LB, augmented when needed by MD results, it is now possible to predict macroscopic transport properties (e.g., permeability) for complex pore networks. The approach has been able to predict quantities that can be measured experimentally and also to predict the hydrocarbon productivity of a given formation or the amount of CO₂ that could be sequestered in a reservoir. When rock formations are particularly heterogeneous, as is the case for many shale formations, it might, however, be impractical to explicitly simulate extremely large rock samples, as for LB approaches to

succeed, it is necessary to explicitly simulate fluid transport through pore networks large enough to represent the elementary pore volume.

Coupling deterministic MD and stochastic KMC simulations

When it is desired to estimate the transport properties of heterogeneous materials, it might be appropriate to implement stochastic methods and estimate the properties of interest for many representations of the pore media, provided that they share some well-identified observables. For example, when porosity, pore size distributions, and mineralogy of a formation are known, one could generate several pore networks with such given characteristics, estimate the transport properties in each representation, and then use appropriate averages for predicting the over-all property of the formation. For such an approach to be feasible, a computationally efficient approach must be available. It is within this scenario that stochastic KMC methods become potentially useful. KMC simulations are often used to stochastically describe transport phenomena controlling various engineering and natural processes.^{153–157} They can access lengthy time scales (from ms to h) and wide spatial dimensions (from nm to μm) at a relatively low computational cost.^{158,159} Fundamentally, KMC takes into consideration state-to-state transition rates to compute trajectories for a system that “wanders” stochastically along the phase space.¹⁵⁹ The KMC implementation requires rate constants that seize the probability per unit

time of state-to-state transitions, which can be obtained from other methods, including MD and LB simulations, and experiments. The order of such transitions creates a sample path or trajectory whose statistics follows the so-called Master equation that determines the dynamics of the system.¹⁵⁹ While the approach has been tested successfully in catalysis,^{154,160–162} its implementation to study transport, including models and algorithms, has been described at length in prior contributions.⁸⁵ KMC allows huge computational savings, compared to MD, as it coarse-grains the molecular trajectories. The energy barrier the system has to overcome in order to get from one energy basin to another determines the waiting time before one event occurs.¹⁵⁹ In a multiscale approach such as represented in Fig. 1, the information of energy barrier could be obtained via atomistic MD studies.

For example, to study fluid transport through a porous medium, Apostolopoulou *et al.*⁸⁵ developed a lattice-based 1D KMC model, which was able to reproduce the atomistic MD simulations conducted by Phan *et al.*²¹ to quantify methane transport through hydrated slit-shaped pores carved out of different solid substrates. Quantitative agreement was achieved between KMC and MD results. Because the KMC model is much more computationally efficient than MD, once the necessary input parameters obtained from MD were appropriately used as a KMC input, it was possible to quantify the contribution of various pore network characteristics to methane transport, including a systematic study on pore length, pore connectivity, and pore width. To quantify the effect of pore width,

Apostolopoulou *et al.*⁸⁷ extended the KMC model to 3D and predicted fluid diffusivity in mesoscale pores carved out of minerals commonly found in shale rocks. The analytical solution of the diffusion equation as well as against a set of atomistic MD results is used to validate the 3D KMC model. Subsequently, the stochastic 3D KMC model was used to estimate the diffusion of pure methane in pores of varying width. Albeit some, rather small deviations were observed between MD and KMC results, the latter method allowed for a systematic quantification of the effect of pore width on the diffusion coefficient of methane, showing that the mineralogy of slit-shaped pores can affect the transport properties of supercritical methane only when the pores are smaller than ~ 3 nm. When the slit pores were wider than ~ 5 nm, the bulk-like diffusion coefficients are predicted for methane diffusing through all the materials considered by Apostolopoulou *et al.*⁸⁷

The lattice KMC model developed by Apostolopoulou *et al.*⁸⁵ can be considered as a bottom-up approach for multi-scale studies. Any fabricated or natural networks can be examined, as long as kinetic (diffusion constants) and thermodynamic (interfacial barriers) properties are available. The latter can, in general, be obtained accurately from MD simulations. It is likely that KMC approaches such as the one just described will provide better insights into the diffusion of multiple components in shale formations and possibly aid the formulation of approaches to enhance the natural gas or oil recovery through shale reservoirs, as well as the permeation of CO₂ in geological formations for permanent sequestration.

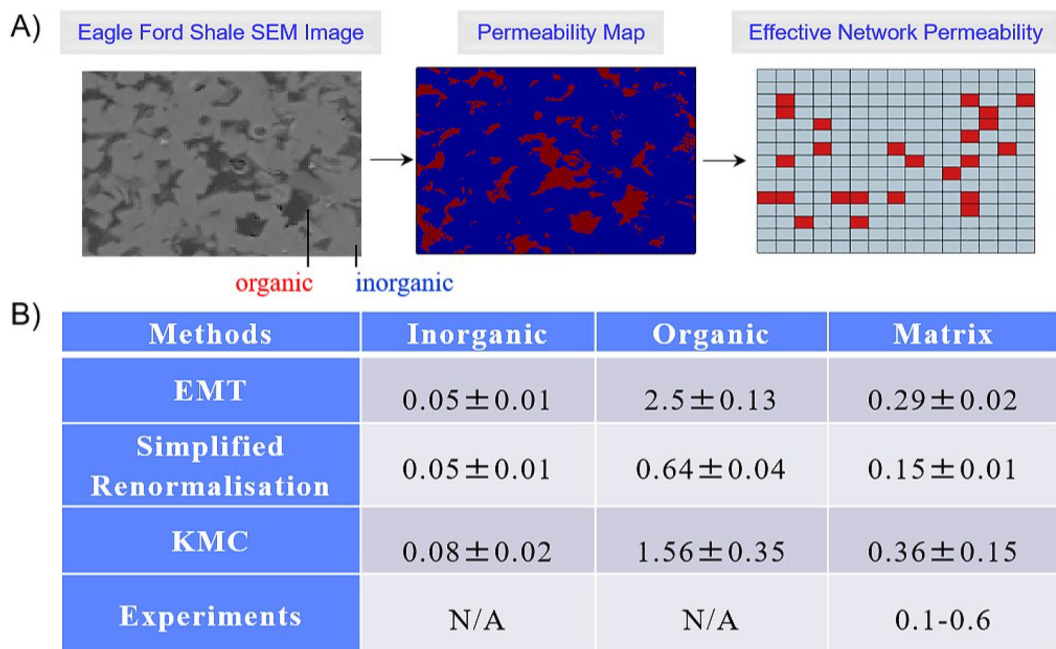


FIG. 7. (a) SEM image of an Eagle Ford sample (left), reproduced with permission from Naraghi and Javadpour, “A stochastic permeability model for the shale-gas systems,” *Int. J. Coal Geol.* **140**, 111–124 (2015). Copyright 2015 Elsevier B.V. Dark gray regions correspond to organic matter and light gray to inorganic matter. Permeability map collected on Eagle Ford samples. An example of the permeability distribution within the matrix networks (organic matter in the inorganic ones). (b) Permeability calculation of the organic and inorganic matter, and the effective network permeability using the effective medium theory (EMT) and simplified renormalization and KMC methods. The organic matter is the high-permeability component. Figures adapted with permission from Ref. 86. Copyright 2019 Elsevier B.V.

To demonstrate the ability of KMC to predict macroscopic quantities, Apostolopoulou *et al.*⁸⁶ used a 2D version of the KMC algorithm to evaluate the permeability of heterogeneous pore networks meant to replicate the properties of shale samples. They compared the KMC approach to the results from the effective medium theory (EMT)¹⁶⁴ and simplified renormalization methods,¹⁶³ which are deterministic approaches often used in practical settings because, in part, of their simplicity. For example, Bhatia and co-workers^{165,166} recently used the EMT to predict effective diffusivities in hierarchical mesoporous zeolite materials. The EMT induces the famous Bruggeman's combination rule,¹⁶⁷ which combines the self-diffusivities for the different domains within the materials in a non-linear fashion. Although the EMT is broadly used, it encounters a few drawbacks, in particular, when many pore blockages exist, and the percolation threshold is approached.¹⁸ Apostolopoulou *et al.*⁸⁶ showed that KMC can accurately account for transitions from low- to high-permeability domains within a material. The most valued characteristic of KMC, compared to the two deterministic methods considered, is its ability to capture anisotropy.⁸⁶ It is therefore expected that KMC could be applicable to low-connectivity networks and

could evaluate the impact of small-scale heterogeneities in which low connectivity exists locally.

When the KMC was used to estimate the permeability of an Eagle Ford shale sample for which data on pore size distributions and one SEM image were available¹⁶³ [see Fig. 7(a)], a reasonable agreement with experimental permeability was achieved using ten stochastic realizations for the inorganic, organic, and dual-permeability networks considered representative of the shale rock [see Fig. 7(b)].^{168–170} While, as shown in Fig. 7, the KMC approach yields results that are broadly consistent with those from EMT and renormalization approaches, it is likely that more pronounced differences will emerge between the three methods when samples more heterogeneous than the one used by Apostolopoulou *et al.* are considered. It is worth noting that the precision of the KMC approach can be enhanced by extending the analysis to more 2D SEM images of a plug sample so that local heterogeneities, anisotropy, and porosity are properly accounted for. It will be challenging to efficiently employ the KMC approach to analyze the permeability of an entire plug sample while taking into account realistic molecular phenomena such as adsorption. The extension of the KMC model to 3D will

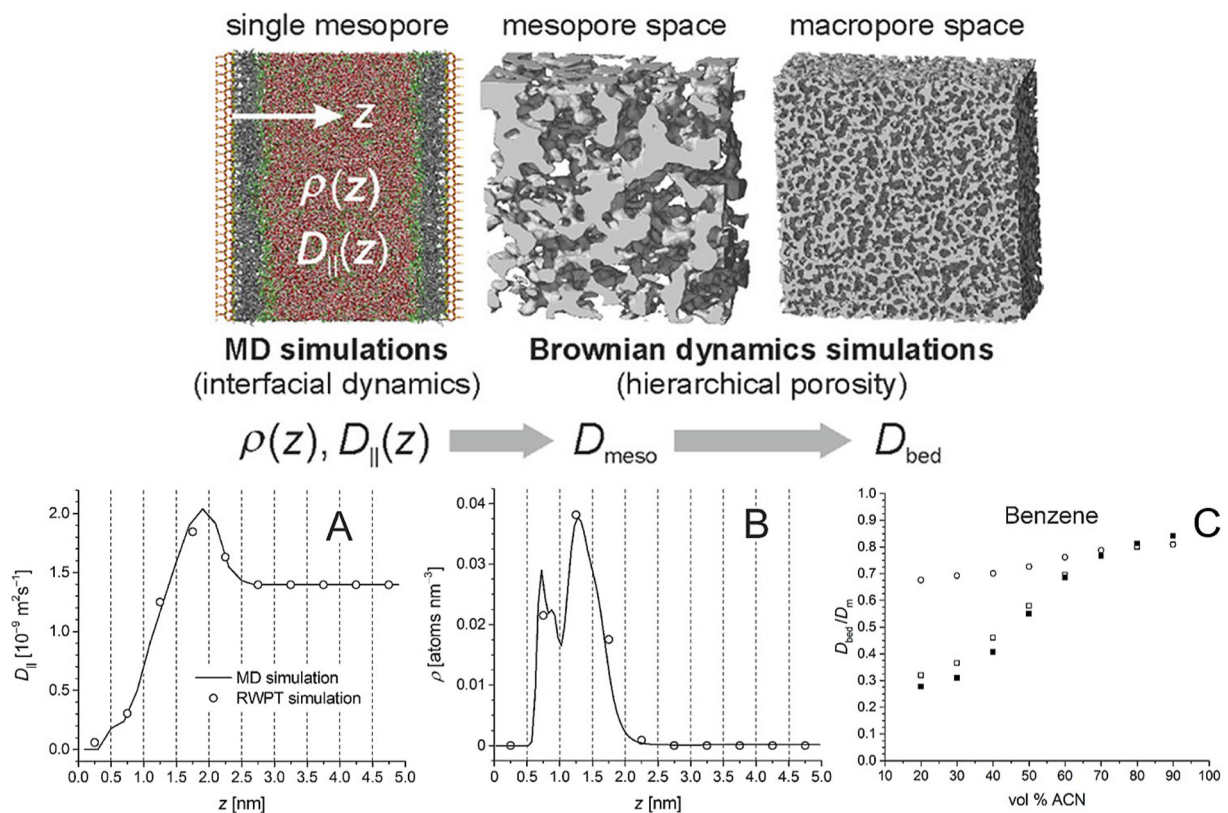


FIG. 8. Top: schematic of a multiscale approach coupling MD and random-walk particle-tracking (RWPT)—Brownian dynamics simulations for calculating bed diffusion coefficients D_{bed} in hierarchically structured, macro/mesoporous materials. Bottom: surface-parallel diffusion coefficient (a) and number density profiles (b) for benzene from MD simulations in the slit-pore model with a mobile phase of water/acetonitrile (solid lines) and from simulations using the RWPT approach (open circles). (c) Effective D_{bed} (normalized by bulk diffusivities D_m) for benzene as a function of the ACN content of the mobile phase. Results were obtained from the presented RWPT approach (solid squares), modified (open squares), and original Maxwell Garnett formula (open circles). Figures adapted with permission from Tallarek *et al.*, "Multiscale simulation of diffusion in porous media: From interfacial dynamics to hierarchical porosity," *J. Phys. Chem. C* **123**(24), 15099–15112 (2019). Copyright 2019 American Chemical Society.

allow for the systematic quantification of the effect of a number of features on the predicted permeability.¹⁷¹

It should be noted, however that it is difficult to obtain some important information on complex pore matrices, such as the connectivity of the 3D pores and some macroscopic properties from 2D SEM images. Newer techniques, e.g., focused ion-beam SEM (FIB-SEM) have been applied to overcome these challenges. For

example, using tomography and FIB-SEM experiments, Botan *et al.*¹⁷² developed a multiscale approach by employing statistical mechanics to study adsorption/transport in porous media while accounting for adsorption in various degrees of porosity. First, a lattice model is built for a given porous solid based on 3D FIB-SEM images with each site representing a porosity domain type, e.g., micro-, meso-, macro-, and non-porous. Subsequently, the

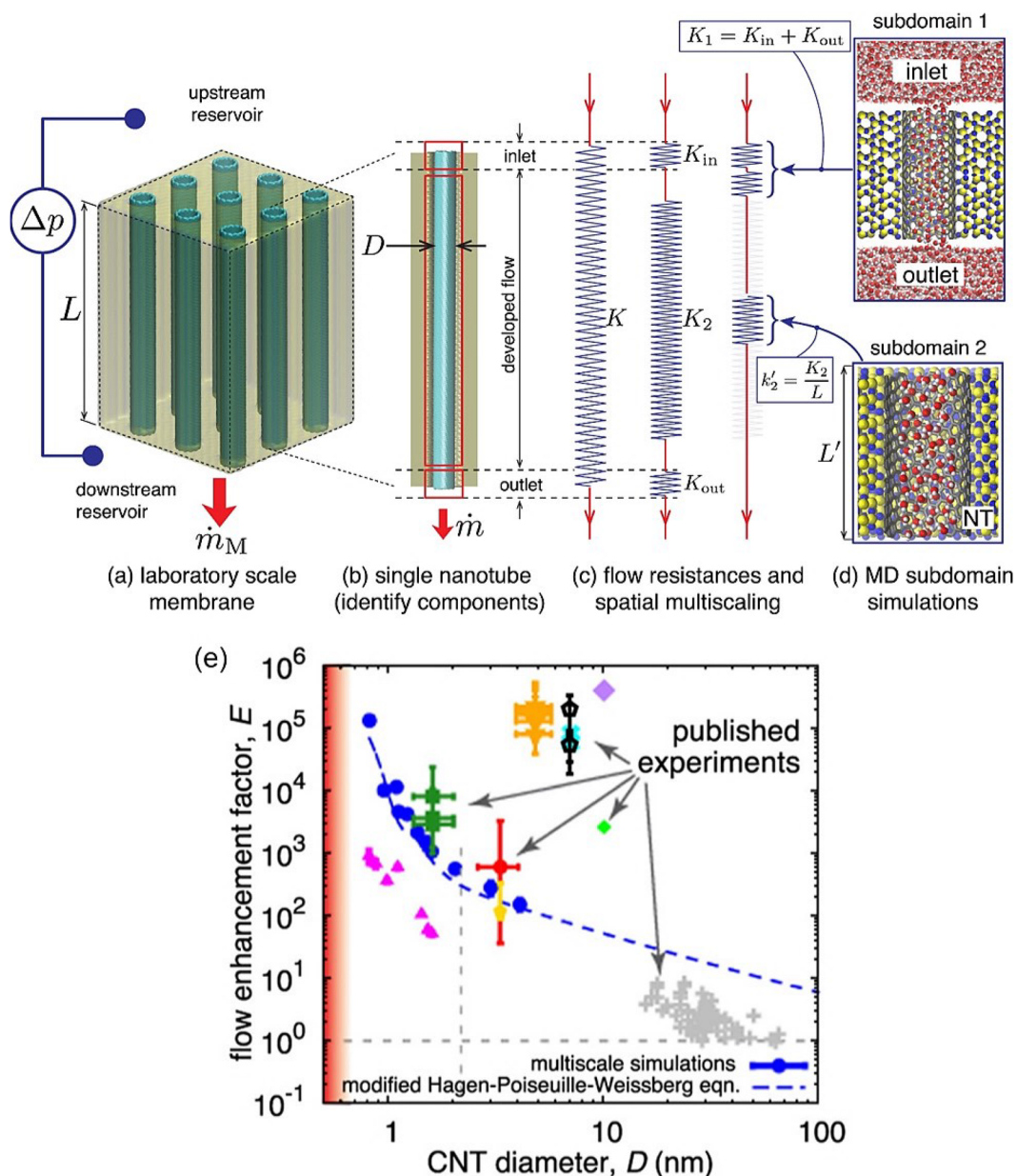


FIG. 9. (a)–(d) Schematic of a multiscale method for modeling flows through laboratory-scale filtration membranes comprising aligned nanotubes. (e) Dependence of the flow enhancement for long CNTs on diameter. Comparisons between the multiscale results (solid blue circles), the calibrated H–P–W equation (blue dashed line), and flow experiments. Figures adapted with permission from Borg *et al.*, “Multiscale simulation of water flow through laboratory-scale nanotube membranes,” *J. Membr. Sci.* **567**, 115–126 (2018). Copyright 2018 Elsevier B.V.

lattice is sketched onto 3D data and the multiscale simulation is conducted to quantify fluid transport as a function of pressure gradient applied across the sample. The advantage of this multiscale model is to enable changes in adsorption and transport upon modifying simulation parameters. In addition, this approach does not require inferring any types of adsorption or flow so that the various phenomena can be taken into consideration. Nevertheless, the extraordinarily small size of samples and the costs for the use of the FIB-SEM technique hinder the broad applicability of the FIB-SEM in characterizing the porous media structure.¹⁷³ Recently, Tahmasebi *et al.*¹⁷⁴ suggested an effective stochastic approach that uses a few 2D images and creates 3D models or realizations of a porous network. It appears that the approach developed by Tahmasebi *et al.*¹⁷⁴ can yield insights into the complexity of shale reservoirs, as well as to other natural porous media with hierarchical pore structures, which could help in improving the accuracy of the KMC method. However, we point out that the accuracy of the stochastic method proposed by Tahmasebi *et al.* depends strongly on the availability of experimental data to reduce the uncertainty in the realizations. Once a representative 3D model is developed, both stochastic and deterministic approaches could be implemented, as discussed in the section titled Coupling MD and other deterministic simulation techniques.

Coupling MD and other deterministic simulation techniques

Tallarek *et al.*¹⁷⁵ presented an attractive bottom-up multiscale simulation approach that is deterministic in nature. Similarly to the work of Apostolopoulou *et al.*,⁸⁷ Tallarek *et al.*¹⁷⁵ derived the effective bed diffusion coefficient (D_{bed}) taking into account for the solute dynamics as well as features such as solute properties, mobile-phase elution strength, and surface chemistry obtained from atomistic MD simulations. This information is incorporated into random-walk particle-tracking (RWPT)^{176,177}—Brownian dynamics (BD) simulations used to extract the effective diffusion coefficient (see Fig. 8, top). In BD simulations, only trajectories and interactions between key particles are computed, while other components of the system are not included explicitly in the simulations but affect indirectly the dynamics of the Brownian particles via a random force. This reduces the dimensionality of the problem, making BD more computationally effective than the corresponding MD simulations.¹⁷⁸ To validate the accuracy of the RWPT approach, Tallarek *et al.*¹⁷⁵ compared the results of benzene diffusivity and density in a slit-pore model with a mixture of water/acetonitrile achieved from MD simulations, showing high levels of consistency. This suggests that the approach is applicable for estimating diffusion in systems with spatially dependent mobility [see Figs. 8(a) and 8(b), bottom]. To harmonize the results of diffusion in hierarchical macro/mesoporosity, Tallarek *et al.*¹⁷⁵ employed the EMT¹⁶⁴ and achieved excellent agreement when comparing D_{bed} against the results from a modified Maxwell Garnett formula developed by Kalnin *et al.*¹⁷⁹ [see Fig. 8(c), bottom]. Similar to the 3D KMC model discussed in the section titled Coupling deterministic MD and stochastic KMC simulations, the multiscale simulation approach proposed by Tallarek *et al.*¹⁷⁵ could strengthen predictive modeling attempts.

Other approaches exist. For example, Borg *et al.* proposed a sequential multiscale simulation method to accurately quantify

macroscopic water flows through laboratory-scale carbon nanotube (CNT) membranes at moderate computational costs.³⁵ The multiscale simulation flow approach combines MD simulations with a continuum fluid model. Figure 9(a) shows an ideal laboratory-scale membrane of thickness L containing many, potentially billions, parallel CNTs. Fluid flow through the membrane can be described as follows: $\Delta p = Km_M$, where K is the flow resistance through an arbitrary CNT and m_M is the steady state mass flow rate through such CNT. The flow model through one CNT is decomposed into three components: one perfect long channel, one entrance, and one exit, as illustrated in Fig. 9(b). The flow resistance K is equivalent to the sum of the three correspondent flow resistances [Fig. 9(c)]. Borg *et al.* conducted one MD simulation for the flow through the combined entrance/exit regions (subdomain 1) and another for the long developed-flow CNT region of length L' (subdomain 2) via applying periodic BCs, as shown in Fig. 9(d). The MD results were then fed as input parameters to a continuum flow model based on the Hagen–Poiseuille–Weissberg (H–P–W) equation.⁷² Subsequently, the generated data are used to correct the H–P–W equation. This approach is easy to implement but still incorporates non-continuum fluid effects. Borg *et al.*³⁵ compared the results of the nanotube flow enhancement factor E as predicted from their H–P–W description against a range of experimental data, as shown in Fig. 9(e). The comparison shows that predictions of Borg *et al.* agree pretty well with some,^{180–182} but not all the literature results.^{183,184} Further studies are needed to resolve the discrepancy. The multiscale computational approach proposed by Borg *et al.*³⁵ appears to be applicable to complex membrane frameworks because it overcomes the drawbacks of the conventional H–P–W formalism, known to be not appropriate for non-ideal configurations.

SUMMARY, CONCLUSIONS, AND PERSPECTIVES

This Review focuses on multiscale fluid transport through heterogeneous porous matrices, with porosity ranging from the molecular (nm) to the macroscopic scale (>micrometer). The increased importance of such complex and multiscale porous materials has raised novel challenges regarding the fundamental understanding of fluid transport through them. In particular, the thermodynamics and dynamics of fluids confined in hierarchical porous media remain somewhat unclear. Among questions left unexplained are the role of interfaces between porosity domains, the breakdown of hydrodynamics at the nanoscale, and the interplay between adsorption and transport mechanisms at each pore scale. Addressing these questions will enable the rational design of hierarchical porous solids for many applications. We have discussed the applicability of each multiscale approach as well with its limitations for modeling fluid transport through heterogeneous porous matrices:

- Atomistic equilibrium/non-equilibrium molecular dynamics (MD) simulations are an efficient technique that reveals a wealth of molecular-detailed properties for confined fluids. However, predicting the transport properties of fluids in hierarchical porous materials consisting of thousands of pores and ultimately within complex pore networks is at present unattainable with MD approaches.
- Fluid transport properties in hierarchical porous materials can be measured by employing appropriate

experimental tools such as pulsed field gradient nuclear magnetic resonance techniques and microimaging; notwithstanding, describing transport in these solids with a general framework remains challenging. Several models such as effective medium theory and simplified renormalization methods have been developed. However, despite significant progress, crucial questions remain to be addressed such as the role of surface energy barriers and the role of gas/liquid interfaces. Such effects can lead to complex activated transport mechanisms that remain poorly understood.

- Lattice Boltzmann (LB) simulations are effective in studying fluid transport at intermediate length and time scales (i.e., the mesoscale) at a modest computational cost. Recent advancements in coupling MD and LB have focused on improving the description of the fluid–substrate and fluid–fluid interactions at the meso-scale.
- Coupling MD and stochastic approaches based on kinetic Monte Carlo with strong connections to experimental characterization of the porous network features have shown the potential of correctly predicting fluid transport in meso- and macro-pores at a large scale while taking into consideration features relevant at different porosity scales, fluid–solid interactions, etc.
- Other approaches based on Brownian dynamics and variations of the continuum Hagen–Poiseuille–Weissberg formalism appear promising for describing complex structures and model membranes, respectively, once the atomistic MD results are used to provide input parameters.

When transport in different porosity scales is well-understood and robust homogenization techniques are developed, prediction of flow through macroscopic pore networks will be achieved using only simple parameters describing the structural features of the porous solid derived using limited datasets and others representing the fluid properties. Such understanding will launch applications in many sectors from energy to catalysis and environmental remediation. It should be stressed that the approach most fruitful for a given application strongly depends on the application itself, as different levels of accuracy are needed to predict, for example, the separation of multicomponent mixtures through a porous membrane or the gas permeability through a heterogeneous rock formation.

ACKNOWLEDGMENTS

Generous allocations of computing time were provided by the ARCHER, the UK National Supercomputing Service (<http://www.archer.ac.uk>) via our membership in the UK's HEC Materials Chemistry Consortium, which is funded by the EPSRC (Grant Nos. EP/L000202 and EP/R029431); the University College London Research Computing Platforms Support (Myriad); the Oklahoma Supercomputing Center for Education and Research (OSCER); and the National Energy Research Scientific Computing Center (NERSC) at the Lawrence Berkeley National Laboratory. The NERSC is supported by the DOE Office of Science under Contract No. DE-AC02-05CH11231. This work was supported, in part, by the Science4CleanEnergy European research consortium funded by the European Union's Horizon 2020 research and innovation programme under Grant Agreement No. 764810 (S4CE).

DATA AVAILABILITY

Data sharing is not applicable to this article as no new data were created or analyzed in this study.

REFERENCES

- ¹J.-D. Grunwaldt, J. B. Wagner, and R. E. Dunin-Borkowski, "Imaging catalysts at work: A hierarchical approach from the macro- to the meso- and nano-scale," *Chemcatchem* **5**(1), 62–80 (2013).
- ²J. Kärger, D. M. Ruthven, and D. N. Theodorou, *Diffusion in Nanoporous Materials* (John Wiley & Sons, Weinheim, 2012).
- ³J. C. S. Remi, A. Lauerer, C. Chmelik, I. Vandendael, H. Terryn, G. V. Baron, J. F. M. Denayer, and J. Kärger, "The role of crystal diversity in understanding mass transfer in nanoporous materials," *Nat. Mater.* **15**(4), 401 (2016).
- ⁴D. Schneider, D. Mehlhorn, P. Zeigermann, J. Kärger, and R. Valiullin, "Transport properties of hierarchical micro-mesoporous materials," *Chem. Soc. Rev.* **45**(12), 3439–3467 (2016).
- ⁵M.-H. Sun, S.-Z. Huang, L.-H. Chen, Y. Li, X.-Y. Yang, Z.-Y. Yuan, and B.-L. Su, "Applications of hierarchically structured porous materials from energy storage and conversion, catalysis, photocatalysis, adsorption, separation, and sensing to biomedicine," *Chem. Soc. Rev.* **45**(12), 3479–3563 (2016).
- ⁶P. Trogadas, V. Ramani, P. Strasser, T. F. Fuller, and M.-O. Coppens, "Hierarchically structured nanomaterials for electrochemical energy conversion," *Angew. Chem., Int. Ed.* **55**(1), 122–148 (2016).
- ⁷L. M. Zhou, K. Zhang, Z. Hu, Z. L. Tao, L. Q. Mai, Y. M. Kang, S. L. Chou, and J. Chen, "Recent developments on and prospects for electrode materials with hierarchical structures for lithium-ion batteries," *Adv. Energy Mater.* **8**(6), 1701415 (2018).
- ⁸D. Cole and A. Striolo, "The influence of nanoporosity on the behavior of carbon-bearing fluids," in *Deep Carbon: Past to Present*, edited by B. Orcutt, I. Daniel, and R. Dasgupta (Cambridge University Press, 2019), pp. 358–387.
- ⁹A. Striolo and D. R. Cole, "Understanding shale gas: Recent progress and remaining challenges," *Energy Fuels* **31**(10), 10300–10310 (2017).
- ¹⁰T. W. Patzek, F. Male, and M. Marder, "Gas production in the Barnett shale obeys a simple scaling theory," *Proc. Natl. Acad. Sci. U. S. A.* **110**(49), 19731–19736 (2013).
- ¹¹T. Müllner, K. K. Unger, and U. Tallarek, "Characterization of microscopic disorder in reconstructed porous materials and assessment of mass transport-relevant structural descriptors," *New J. Chem.* **40**(5), 3993–4015 (2016).
- ¹²I. I. Ivanova and E. E. Knyazeva, "Micro-mesoporous materials obtained by zeolite recrystallization: Synthesis, characterization and catalytic applications," *Chem. Soc. Rev.* **42**(9), 3671–3688 (2013).
- ¹³A. Inayat, B. Reinhardt, H. Uhlig, W.-D. Einicke, and D. Enke, "Silica monoliths with hierarchical porosity obtained from porous glasses," *Chem. Soc. Rev.* **42**(9), 3753–3764 (2013).
- ¹⁴A. Sachse, A. Galarneau, F. Fajula, F. Di Renzo, P. Creux, and B. Coq, "Functional silica monoliths with hierarchical uniform porosity as continuous flow catalytic reactors," *Microporous Mesoporous Mater.* **140**(1–3), 58–68 (2011).
- ¹⁵P. Innocenzi, L. Malfatti, and G. J. A. A. Soler-Illia, "Hierarchical mesoporous films: From self-assembly to porosity with different length scales," *Chem. Mater.* **23**(10), 2501–2509 (2011).
- ¹⁶A. Sachse, R. Ameloot, B. Coq, F. Fajula, B. Coasne, D. De Vos, and A. Galarneau, "In situ synthesis of Cu-BTC (HKUST-1) in macro-/mesoporous silica monoliths for continuous flow catalysis," *Chem. Commun.* **48**(39), 4749–4751 (2012).
- ¹⁷A. Phan and A. Striolo, "Methane transport through hierarchical silica micro-mesoporous materials: From non-equilibrium atomistic simulations to phenomenological correlations," *Microporous Mesoporous Mater.* **288**, 109559 (2019).
- ¹⁸B. Coasne, "Multiscale adsorption and transport in hierarchical porous materials," *New J. Chem.* **40**(5), 4078–4094 (2016).
- ¹⁹T. Bui, A. Phan, D. R. Cole, and A. Striolo, "Transport mechanism of guest methane in water-filled nanopores," *J. Phys. Chem. C* **121**(29), 15675–15686 (2017).

- ²⁰D. Hlushkou, F. Gritti, A. Daneyko, G. Guiochon, and U. Tallarek, "How microscopic characteristics of the adsorption kinetics impact macroscale transport in chromatographic beds," *J. Phys. Chem. C* **117**(44), 22974–22985 (2013).
- ²¹A. Phan, D. R. Cole, R. G. Weiss, J. Dzubiella, and A. Striolo, "Confined water determines transport properties of guest molecules in narrow pores," *ACS Nano* **10**(8), 7646–7656 (2016).
- ²²J. D. Evans, G. Fraux, R. Gaillac, D. Kohen, F. Trouselet, J.-M. Vanson, and F.-X. Coudert, "Computational chemistry methods for nanoporous materials," *Chem. Mater.* **29**(1), 199–212 (2017).
- ²³T. Le, A. Striolo, and D. R. Cole, "CO₂-C₄H₁₀ mixtures simulated in silica slit pores: Relation between structure and dynamics," *J. Phys. Chem. C* **119**(27), 15274–15284 (2015).
- ²⁴S. Gautam, T. Le, A. Striolo, and D. Cole, "Molecular dynamics simulations of propane in slit shaped silica nano-pores: Direct comparison with quasielastic neutron scattering experiments," *Phys. Chem. Chem. Phys.* **19**(48), 32320–32332 (2017).
- ²⁵T. T. B. Le, A. Striolo, S. S. Gautam, and D. R. Cole, "Propane-water mixtures confined within cylindrical silica nanopores: Structural and dynamical properties probed by molecular dynamics," *Langmuir* **33**(42), 11310–11320 (2017).
- ²⁶S. T. O'Connell and P. A. Thompson, "Molecular dynamics-continuum hybrid computations: A tool for studying complex fluid flows," *Phys. Rev. E* **52**(6), R5792–R5795 (1995).
- ²⁷J.-F. Bourgat, P. LeTallec, and M. D. Tidriri, "Coupling Boltzmann and Navier-Stokes equations by friction," *J. Comput. Phys.* **127**(2), 227–245 (1996).
- ²⁸V. B. Shenoy, R. Miller, E. B. Tadmor, R. Phillips, and M. Ortiz, "Quasi-continuum models of interfacial structure and deformation," *Phys. Rev. Lett.* **80**(4), 742–745 (1998).
- ²⁹A. Galarneau, F. Villemot, J. Rodriguez, F. Fajula, and B. Coasne, "Validity of the t-plot method to assess microporosity in hierarchical micro/mesoporous materials," *Langmuir* **30**(44), 13266–13274 (2014).
- ³⁰B. Coasne, A. Galarneau, C. Gerardin, F. Fajula, and F. Villemot, "Molecular simulation of adsorption and transport in hierarchical porous materials," *Langmuir* **29**(25), 7864–7875 (2013).
- ³¹A. Ledesma-Durán, S. I. H. Hernández, and I. Santamaría-Holek, "Effectiveness factor and mass transfer coefficient in wedge and funnel pores using a generalized Fick-Jacobs model," *J. Phys. Chem. C* **120**(51), 29153–29161 (2016).
- ³²E. Bjornehohn, M. H. Hansen, A. Hodgson, L. M. Liu, D. T. Limmer, A. Michaelides, P. Pedevilla, J. Rossmel, H. Shen, G. Tocci, E. Tyrode, M. M. Walz, J. Werner, and H. Blumh, "Water at interfaces," *Chem. Rev.* **116**(13), 7698–7726 (2016).
- ³³I. N. Tsimpanogiannis, O. A. Moutlos, L. F. M. Franco, M. B. D. Spera, M. Erdos, and I. G. Economou, "Self-diffusion coefficient of bulk and confined water: A critical review of classical molecular simulation studies," *Mol. Simul.* **45**(4–5), 425–453 (2019).
- ³⁴R. J. Kirkpatrick, A. G. Kalinichev, G. M. Bowers, A. Ö. Yazaydin, M. Krishnan, M. Saharay, and C. P. Morrow, "NMR and computational molecular modeling studies of mineral surfaces and interlayer galleries: A review," *Am. Mineral.* **100**(7), 1341–1354 (2015).
- ³⁵M. K. Borg, D. A. Lockerby, K. Ritos, and J. M. Reese, "Multiscale simulation of water flow through laboratory-scale nanotube membranes," *J. Membr. Sci.* **567**, 115–126 (2018).
- ³⁶D. Vlachos, "A review of multiscale Analysis: Examples from systems biology, materials engineering, and other fluid-surface interacting systems," *Adv. Chem. Eng.* **30**, 1–61 (2004).
- ³⁷A. Galarneau, F. Guenneau, A. Gedeon, D. Mereib, J. Rodriguez, F. Fajula, and B. Coasne, "Probing interconnectivity in hierarchical microporous/mesoporous materials using adsorption and nuclear magnetic resonance diffusion," *J. Phys. Chem. C* **120**(3), 1562–1569 (2016).
- ³⁸J. Kärger and R. Valiullin, "Mass transfer in mesoporous materials: The benefit of microscopic diffusion measurement," *Chem. Soc. Rev.* **42**(9), 4172–4197 (2013).
- ³⁹C. Chmelik, D. Enke, P. Galvosas, O. Gobin, A. Jentys, H. Jobic, J. Kärger, C. B. Krause, J. Kullmann, J. Lercher, S. Naumov, D. M. Ruthven, and T. Titz, "Nanoporous glass as a model system for a consistency check of the different techniques of diffusion measurement," *Chemphyschem* **12**(6), 1130–1134 (2011).
- ⁴⁰H. Jobic and D. N. Theodorou, "Quasi-elastic neutron scattering and molecular dynamics simulation as complementary techniques for studying diffusion in zeolites," *Microporous Mesoporous Mater.* **102**(1–3), 21–50 (2007).
- ⁴¹J. Kärger, T. Binder, C. Chmelik, F. Hibbe, H. Krautscheid, R. Krishna, and J. Weitkamp, "Microimaging of transient guest profiles to monitor mass transfer in nanoporous materials," *Nat. Mater.* **13**(4), 333–343 (2014).
- ⁴²J. Kärger, "Transport phenomena in nanoporous materials," *Chemphyschem* **16**(1), 24–51 (2015).
- ⁴³A. Lauerer, P. Zeigermann, J. Lenzner, C. Chmelik, M. Thommes, R. Valiullin, and J. Kärger, "Micro-imaging of liquid-vapor phase transition in nano-channels," *Microporous Mesoporous Mater.* **214**, 143–148 (2015).
- ⁴⁴N. Loganathan, G. M. Bowers, B. F. N. Wakou, A. G. Kalinichev, R. J. Kirkpatrick, and A. O. Yazaydin, "Understanding methane/carbon dioxide partitioning in clay nano- and meso-pores with constant reservoir composition molecular dynamics modeling," *Phys. Chem. Chem. Phys.* **21**(13), 6917–6924 (2019).
- ⁴⁵S. Patankar, S. Gautam, G. Rother, A. Podlesnyak, G. Ehlers, T. Liu, D. R. Cole, and D. L. Tomasko, "Role of confinement on adsorption and dynamics of ethane and an ethane-CO₂ mixture in mesoporous CPG silica," *J. Phys. Chem. C* **120**(9), 4843–4853 (2016).
- ⁴⁶N. Loganathan, A. O. Yazaydin, G. M. Bowers, A. G. Kalinichev, and R. J. Kirkpatrick, "Molecular dynamics study of CO₂ and H₂O intercalation in smectite clays: Effect of temperature and pressure on interlayer structure and dynamics in hectorite," *J. Phys. Chem. C* **121**(44), 24527–24540 (2017).
- ⁴⁷R. Radhakrishnan, K. E. Gubbins, and M. Sliwinski-Bartkowiak, "Existence of a hexatic phase in porous media," *Phys. Rev. Lett.* **89**(7), 076101 (2002).
- ⁴⁸C. Perego, M. Salvalaglio, and M. Parrinello, "Molecular dynamics simulations of solutions at constant chemical potential," *J. Chem. Phys.* **142**(14), 144113 (2015).
- ⁴⁹A. Ozcan, C. Perego, M. Salvalaglio, M. Parrinello, and O. Yazaydin, "Concentration gradient driven molecular dynamics: A new method for simulations of membrane permeation and separation," *Chem. Sci.* **8**(5), 3858–3865 (2017).
- ⁵⁰M. P. Allen and D. J. Tildesley, *Computer Simulation of Liquids* (Oxford University Press, Oxford, UK, 2004).
- ⁵¹J. F. Xie, M. K. Borg, L. Gibelli, O. Henrich, D. A. Lockerby, and J. M. Reese, "Effective mean free path and viscosity of confined gases," *Phys. Fluids* **31**(7), 072002 (2019).
- ⁵²T. Le, S. Ogbe, A. Striolo, and D. R. Cole, "N-octane diffusivity enhancement via carbon dioxide in silica slit-shaped nanopores - a molecular dynamics simulation," *Mol. Simul.* **42**(9), 745–752 (2016).
- ⁵³S. Gautam, T. Liu, G. Rother, N. Jalarvo, E. Mamontov, S. Welch, J. Sheets, M. Droege, and D. R. Cole, "Dynamics of propane in nanoporous silica aerogel: A quasielastic neutron scattering study," *J. Phys. Chem. C* **119**(32), 18188–18195 (2015).
- ⁵⁴S. M. Chathoth, L. He, E. Mamontov, and Y. B. Melnichenko, "Effect of carbon dioxide and nitrogen on the diffusivity of methane confined in nano-porous carbon aerogel," *Microporous Mesoporous Mater.* **148**(1), 101–106 (2012).
- ⁵⁵S. Boinepalli and P. Attard, "Grand canonical molecular dynamics," *J. Chem. Phys.* **119**(24), 12769–12775 (2003).
- ⁵⁶S. Gautam, T. T. B. Le, G. Rother, N. Jalarvo, T. Liu, E. Mamontov, S. Dai, Z.-A. Qiao, A. Striolo, and D. Cole, "Effects of water on the stochastic motions of propane confined in MCM-41-S pores," *Phys. Chem. Chem. Phys.* **21**(45), 25035–25046 (2019).
- ⁵⁷Y. Hu, M. Li, G. Hou, S. Xu, K. Gong, X. Liu, X. Han, X. Pan, and X. Bao, "The role of water in methane adsorption and diffusion within nanoporous silica investigated by hyperpolarized ¹²⁹Xe and ¹H PFG NMR spectroscopy," *Nano Res.* **11**(1), 360–369 (2018).
- ⁵⁸T. A. Ho, Y. Wang, A. Ilgen, L. J. Criscenti, and C. M. Tenney, "Supercritical CO₂-induced atomistic lubrication for water flow in a rough hydrophilic nanochannel," *Nanoscale* **10**(42), 19957–19963 (2018).
- ⁵⁹T. A. Ho and Y. Wang, "Enhancement of oil flow in shale nanopores by manipulating friction and viscosity," *Phys. Chem. Chem. Phys.* **21**(24), 12777–12786 (2019).
- ⁶⁰T. A. Ho and Y. Wang, "Pore size effect on selective gas transport in shale nanopores," *J. Nat. Gas Sci. Eng.* **83**, 103543 (2020).

- ⁶¹H. Frentrup, C. Avendaño, M. Horsch, A. Salih, and E. A. Müller, "Transport diffusivities of fluids in nanopores by non-equilibrium molecular dynamics simulation," *Mol. Simul.* **38**(7), 540–553 (2012).
- ⁶²J. Muscatello, F. Jaeger, O. K. Matar, and E. A. Müller, "Optimizing water transport through graphene-based membranes: Insights from nonequilibrium molecular dynamics," *ACS Appl. Mater. Interfaces* **8**(19), 12330–12336 (2016).
- ⁶³T. Wu and A. Firoozabadi, "Molecular simulations of binary gas mixture transport and separation in slit nanopores," *J. Phys. Chem. C* **122**(36), 20727–20735 (2018).
- ⁶⁴A. Nalaparaju, J. Wang, and J. Jiang, "Enhancing water permeation through alumina membranes by changing from cylindrical to conical nanopores," *Nanoscale* **11**(20), 9869–9878 (2019).
- ⁶⁵F. A. Cabrales-Navarro, J. L. Gómez-Ballesteros, and P. B. Balbuena, "Molecular dynamics simulations of metal-organic frameworks as membranes for gas mixtures separation," *J. Membr. Sci.* **428**, 241–250 (2013).
- ⁶⁶K. Mizukami, H. Takaba, Y. Kobayashi, Y. Oumi, R. V. Belosludov, S. Takami, M. Kubo, and A. Miyamoto, "Molecular dynamics calculations of CO₂/N₂ mixture through the NaY type zeolite membrane," *J. Membr. Sci.* **188**(1), 21–28 (2001).
- ⁶⁷A. Phan and A. Striolo, "Evidence of facilitated transport in crowded nanopores," *J. Phys. Chem. Lett.* **11**(5), 1814–1821 (2020).
- ⁶⁸Y. An, S. M. Althaus, H.-H. Liu, and J.-H. Chen, "Nuclear magnetic resonance measurement of methane diffusion in organic-rich shales," *Fuel* **247**, 160–163 (2019).
- ⁶⁹K. Falk, B. Coasne, R. Pellenq, F. J. Ulm, and L. Bocquet, "Subcontinuum mass transport of condensed hydrocarbons in nanoporous media," *Nat. Commun.* **6**, 6949 (2015).
- ⁷⁰S. P. Neuman, "Theoretical derivation of Darcy's law," *Acta Mech.* **25**, 153–170 (1977).
- ⁷¹M. E. Suk and N. R. Aluru, "Modeling water flow through carbon nanotube membranes with entrance/exit effects," *Nanoscale Microscale Thermophys. Eng.* **21**(4), 247–262 (2017).
- ⁷²J. H. Walther, K. Ritos, E. R. Cruz-Chu, C. M. Megaridis, and P. Koumoutsakos, "Barriers to superfast water transport in carbon nanotube membranes," *Nano Lett.* **13**(5), 1910–1914 (2013).
- ⁷³H. L. Weissberg, "End correction for slow viscous flow through long tubes," *Phys. Fluids* **5**(9), 1033–1036 (1962).
- ⁷⁴D. M. Holland, D. A. Lockerby, M. K. Borg, W. D. Nicholls, and J. M. Reese, "Molecular dynamics pre-simulations for nanoscale computational fluid dynamics," *Microfluid. Nanofluid.* **18**(3), 461–474 (2015).
- ⁷⁵B. Ghanbarian, A. G. Hunt, R. P. Ewing, and M. Sahimi, "Tortuosity in porous media: A critical review," *Soil Sci. Soc. Am. J.* **77**(5), 1461–1477 (2013).
- ⁷⁶A. Ledesma-Duran, S. I. Hernandez, and I. Santamaria-Holek, "Relation between the porosity and tortuosity of a membrane formed by disconnected irregular pores and the spatial diffusion coefficient of the Fick–Jacobs model," *Phys. Rev. E* **95**(5), 052804 (2017).
- ⁷⁷N. R. Backeberg, F. Iacoviello, M. Rittner, T. M. Mitchell, A. P. Jones, R. Day, J. Wheeler, P. R. Shearing, P. Vermeesch, and A. Striolo, "Quantifying the anisotropy and tortuosity of permeable pathways in clay-rich mudstones using models based on X-ray tomography," *Sci Rep* **7**, 14838 (2017).
- ⁷⁸C. F. Berg, "Permeability description by characteristic length, tortuosity, constriction and porosity," *Transp. Porous Media* **103**(3), 381–400 (2014).
- ⁷⁹C. H. Arns, M. A. Knackstedt, W. V. Pinczewski, and N. S. Martys, "Virtual permeametry on microtomographic images," *J. Pet. Sci. Eng.* **45**(1–2), 41–46 (2004).
- ⁸⁰A. Vishnyakov, R. Mao, M. T. Lee, and A. V. Neimark, "Coarse-grained model of nanoscale segregation, water diffusion, and proton transport in Nafion membranes," *J. Chem. Phys.* **148**(2), 024108 (2018).
- ⁸¹K. Zhang, D. Meng, F. Müller-Plathe, and S. K. Kumar, "Coarse-grained molecular dynamics simulation of activated penetrant transport in glassy polymers," *Soft Matter* **14**(3), 440–447 (2018).
- ⁸²M. Levesque, M. Duvaal, I. Pagonabarraga, D. Frenkel, and B. Rotenberg, "Accounting for adsorption and desorption in lattice Boltzmann simulations," *Phys. Rev. E* **88**(1), 013308 (2013).
- ⁸³J.-M. Vanson, F.-X. Coudert, B. Rotenberg, M. Levesque, C. Tardivat, M. Klotz, and A. Boutin, "Unexpected coupling between flow and adsorption in porous media," *Soft Matter* **11**(30), 6125–6133 (2015).
- ⁸⁴D. Fan, A. Phan, and A. Striolo, "Accurate permeability prediction in tight gas rocks via lattice Boltzmann simulations with an improved boundary condition," *J. Nat. Gas Sci. Eng.* **73**, 103049 (2020).
- ⁸⁵M. Apostolopoulou, R. Day, R. Hull, M. Stamatakis, and A. Striolo, "A kinetic Monte Carlo approach to study fluid transport in pore networks," *J. Chem. Phys.* **147**(13), 134703 (2017).
- ⁸⁶M. Apostolopoulou, R. Dusterhoft, R. Day, M. Stamatakis, M.-O. Coppens, and A. Striolo, "Estimating permeability in shales and other heterogeneous porous media: Deterministic vs. stochastic investigations," *Int. J. Coal Geol.* **205**, 140–154 (2019).
- ⁸⁷M. Apostolopoulou, M. S. Santos, M. Hamza, T. Bui, I. G. Economou, M. Stamatakis, and A. Striolo, "Quantifying pore width effects on diffusivity via a novel 3D stochastic approach with input from atomistic molecular dynamics simulations," *J. Chem. Theory Comput.* **15**(12), 6907–6922 (2019).
- ⁸⁸M. Sega, M. Sbragaglia, S. S. Kantorovich, and A. O. Ivanov, "Mesoscale structures at complex fluid–fluid interfaces: A novel lattice Boltzmann/molecular dynamics coupling," *Soft Matter* **9**(42), 10092 (2013).
- ⁸⁹T. Krüger, H. Kusumaatmaja, A. Kuzmin, O. Shardt, G. Silva, and E. M. Viggen, *The Lattice Boltzmann Method* (Springer International Publishing, Cham, 2017), p. 705.
- ⁹⁰O. Mahian, L. Kolsi, M. Amani, P. Estellé, G. Ahmadi, C. Kleinstreuer, J. S. Marshall, R. A. Taylor, E. Abu-Nada, S. Rashidi, H. Niazmand, S. Wongwises, T. Hayat, A. Kasaeian, and I. Pop, "Recent advances in modeling and simulation of nanofluid flows-Part II: Fundamentals and theory," *Phys. Rep.* **791**, 1–59 (2019).
- ⁹¹Y. Feng, S. Guo, J. Jacob, and P. Sagaut, "Solid wall and open boundary conditions in hybrid recursive regularized lattice Boltzmann method for compressible flows," *Phys. Fluids* **31**(12), 126103 (2019).
- ⁹²Y. Kim, H. Choi, Y. G. Park, J. Jang, and M. Y. Ha, "Numerical study on the immiscible two-phase flow in a nano-channel using a molecular-continuum hybrid method," *J. Mech. Sci. Technol.* **33**(9), 4291–4302 (2019).
- ⁹³M. A. A. Spaid and F. R. Phelan, Jr., "Lattice Boltzmann methods for modeling microscale flow in fibrous porous media," *Phys. Fluids* **9**(9), 2468–2474 (1997).
- ⁹⁴Z. Guo and C. Shu, *Lattice Boltzmann Method and its Applications in Engineering* (World Scientific: Hackensack, New Jersey, 2013), Vol. 3, p. xiii.
- ⁹⁵R. Benzi, L. Biferale, M. Sbragaglia, S. Succi, and F. Toschi, "Mesoscopic modelling of fluid flows in micro and nano channel," *Int. J. Mod. Phys. C* **18**(04), 758–765 (2007).
- ⁹⁶Y.-L. He and W.-Q. Tao, "Numerical solutions of nano/microphenomena coupled with macroscopic process of heat transfer and fluid flow: A brief review," *J. Heat Transfer* **137**(9), 090801 (2015).
- ⁹⁷D. Raabe, "Overview of the lattice Boltzmann method for nano- and microscale fluid dynamics in materials science and engineering," *Modell. Simul. Mater. Sci. Eng.* **12**(6), R13–R46 (2004).
- ⁹⁸J. Zhang, "Lattice Boltzmann method for microfluidics: Models and applications," *Microfluid. Nanofluid.* **10**(1), 1–28 (2011).
- ⁹⁹J. Wang, L. Chen, Q. Kang, and S. S. Rahman, "The lattice Boltzmann method for isothermal micro-gaseous flow and its application in shale gas flow: A review," *Int. J. Heat Mass Transfer* **95**, 94–108 (2016).
- ¹⁰⁰M. Wörner, "Numerical modeling of multiphase flows in microfluidics and micro process engineering: A review of methods and applications," *Microfluid. Nanofluid.* **12**(6), 841–886 (2012).
- ¹⁰¹A. Dupuis, E. M. Kotsalis, and P. Koumoutsakos, "Coupling lattice Boltzmann and molecular dynamics models for dense fluids," *Phys. Rev. E* **75**(4), 046704 (2007).
- ¹⁰²R. Verberg, C. M. Pooley, J. M. Yeomans, and A. C. Balazs, "Pattern formation in binary fluids confined between rough, chemically heterogeneous surfaces," *Phys. Rev. Lett.* **93**(18), 184501 (2004).
- ¹⁰³S. Chibbaro, E. Costa, D. I. Dimitrov, F. Diotallevi, A. Milchev, D. Palmieri, G. Pontrelli, and S. Succi, "Capillary filling in microchannels with wall corrugations: A comparative study of the Concus–Finn criterion by continuum, kinetic, and atomistic approaches," *Langmuir* **25**(21), 12653–12660 (2009).

- ¹⁰⁴S. Chakraborty, "Order parameter modeling of fluid dynamics in narrow confinements subjected to hydrophobic interactions," *Phys. Rev. Lett.* **99**(9), 094504 (2007).
- ¹⁰⁵Y. Zhang, R. Qin, and D. R. Emerson, "Lattice Boltzmann simulation of rarefied gas flows in microchannels," *Phys. Rev. E* **71**(4 Pt 2), 047702 (2005).
- ¹⁰⁶E. Fathi and I. Y. Akkutlu, "Lattice Boltzmann method for simulation of shale gas transport in kerogen," *SPE J.* **18**(01), 27–37 (2012).
- ¹⁰⁷Y. Wang and S. A. Aryana, "Pore-scale simulation of gas flow in microscopic permeable media with complex geometries," *J. Nat. Gas Sci. Eng.* **81**, 103441 (2020).
- ¹⁰⁸Y. Ning, Y. Jiang, H. Liu, and G. Qin, "Numerical modeling of slippage and adsorption effects on gas transport in shale formations using the lattice Boltzmann method," *J. Nat. Gas Sci. Eng.* **26**, 345–355 (2015).
- ¹⁰⁹L. Chen, L. Zhang, Q. Kang, H. S. Viswanathan, J. Yao, and W. Tao, "Nanoscale simulation of shale transport properties using the lattice Boltzmann method: Permeability and diffusivity," *Sci. Rep.* **5**(1), 8089 (2015).
- ¹¹⁰H. Yu, J. Chen, Y. Zhu, F. Wang, and H. Wu, "Multiscale transport mechanism of shale gas in micro/nano-pores," *Int. J. Heat Mass Transfer* **111**, 1172–1180 (2017).
- ¹¹¹J. Harting, C. Kunert, and H. J. Herrmann, "Lattice Boltzmann simulations of apparent slip in hydrophobic microchannels," *Europhys. Lett.* **75**(2), 328–334 (2006).
- ¹¹²S. Chibbaro, L. Biferale, F. Diotallevi, S. Succi, K. Binder, D. Dimitrov, A. Milchev, S. Girardo, and D. Pisignano, "Evidence of thin-film precursors formation in hydrokinetic and atomistic simulations of nano-channel capillary filling," *Europhys. Lett.* **84**(4), 44003 (2008).
- ¹¹³J. Horbach and S. Succi, "Lattice Boltzmann versus molecular dynamics simulation of nanoscale hydrodynamic flows," *Phys. Rev. Lett.* **96**(22), 224503 (2006).
- ¹¹⁴S. Succi, A. A. Mohammad, and J. Horbach, "Lattice-Boltzmann simulation of dense nanoflows: A comparison with molecular dynamics and Navier–Stokes solutions," *Int. J. Mod. Phys. C* **18**(04), 667–675 (2007).
- ¹¹⁵H. Yoshida and L. Bocquet, "Labyrinthine water flow across multilayer graphene-based membranes: Molecular dynamics versus continuum predictions," *J. Chem. Phys.* **144**(23), 234701 (2016).
- ¹¹⁶S. Chen, M. Wang, and Z. Xia, "Multiscale fluid mechanics and modeling," *Procedia IUTAM* **10**, 100–114 (2014).
- ¹¹⁷P. Neumann, H. Flohr, R. Arora, P. Jarmatz, N. Tchipev, and H.-J. Bungartz, "MaMiCo: Software design for parallel molecular-continuum flow simulations," *Comput. Phys. Commun.* **200**, 324–335 (2016).
- ¹¹⁸S. K. Saha and G. P. Celata, "Advances in modelling of biomimetic fluid flow at different scales," *Nanoscale Res. Lett.* **6**, 344 (2011).
- ¹¹⁹J. Zhao, Q. Kang, J. Yao, L. Zhang, Z. Li, Y. Yang, and H. Sun, "Lattice Boltzmann simulation of liquid flow in nanoporous media," *Int. J. Heat Mass Transfer* **125**, 1131–1143 (2018).
- ¹²⁰T. Zhang, X. Li, Y. Yin, M. He, Q. Liu, L. Huang, and J. Shi, "The transport behaviors of oil in nanopores and nanoporous media of shale," *Fuel* **242**, 305–315 (2019).
- ¹²¹P. Hou, Y. Ju, F. Gao, J. Wang, and J. He, "Simulation and visualization of the displacement between CO₂ and formation fluids at pore-scale levels and its application to the recovery of shale gas," *Int. J. Coal Sci. Technol.* **3**(4), 351–369 (2016).
- ¹²²X. Liu, Y.-F. Zhu, B. Gong, J.-P. Yu, and S.-T. Cui, "From molecular dynamics to lattice Boltzmann: A new approach for pore-scale modeling of multi-phase flow," *Pet. Sci.* **12**(2), 282–292 (2015).
- ¹²³Z.-Z. Li, T. Min, Q. Kang, Y.-L. He, and W.-Q. Tao, "Investigation of methane adsorption and its effect on gas transport in shale matrix through microscale and mesoscale simulations," *Int. J. Heat Mass Transfer* **98**, 675–686 (2016).
- ¹²⁴K. Suga, S. Takenaka, T. Ito, and M. Kaneda, "Lattice Boltzmann flow simulation in a combined nanochannel," *Adv. Appl. Math. Mech.* **2**, 609–625 (2010).
- ¹²⁵K. Suga, "Lattice Boltzmann methods for complex micro-flows: Applicability and limitations for practical applications," *Fluid Dyn. Res.* **45**(3), 034501 (2013).
- ¹²⁶K. Suga, S. Takenaka, T. Ito, M. Kaneda, T. Kinjo, and S. Hyodo, "Evaluation of a lattice Boltzmann method in a complex nanoflow," *Phys. Rev. E* **82**(1 Pt 2), 016701 (2010).
- ¹²⁷J. Zhao, J. Yao, M. Zhang, L. Zhang, Y. Yang, H. Sun, S. An, and A. Li, "Study of gas flow characteristics in tight porous media with a microscale lattice Boltzmann model," *Sci. Rep.* **6**, 32393 (2016).
- ¹²⁸H. Zuo, S. Deng, and H. Li, "Limitations of lattice Boltzmann modeling of micro-flows in complex nanopores," *Acta Geol. Sin. (Engl. Ed.)* **93**(6), 1808–1822 (2019).
- ¹²⁹J. Meng, X.-J. Gu, and D. R. Emerson, "Analysis of non-physical slip velocity in lattice Boltzmann simulations using the bounce-back scheme," *J. Comput. Sci.* **28**, 476–482 (2018).
- ¹³⁰R. N. Moghaddam and M. Jamiolahmady, "Study of slip flow in unconventional shale rocks using lattice Boltzmann method: Effects of boundary conditions and TMAC," *Transp. Porous Media* **120**(1), 115–139 (2017).
- ¹³¹A. S. Ziarani and R. Aguilera, "Knudsen's permeability correction for tight porous media," *Transp. Porous Media* **91**(1), 239–260 (2012).
- ¹³²A. Velasco, S. Friedman, M. Pevarnik, Z. Siwy, and P. Taborek, "Pressure-driven flow through a single nanopore," *Phys. Rev. E* **86**(2), 025302 (2012).
- ¹³³A. Beskok and G. E. Karniadakis, "Report: A model for flows in channels, pipes, and ducts at micro and nano scales," *Microscale Thermophys. Eng.* **3**(1), 43–77 (1999).
- ¹³⁴F. Civan, "Effective correlation of apparent gas permeability in tight porous media," *Transp. Porous Media* **82**(2), 375–384 (2010).
- ¹³⁵S. Chen, D. Martínez, and R. Mei, "On boundary conditions in lattice Boltzmann methods," *Phys. Fluids* **8**(9), 2527–2536 (1996).
- ¹³⁶O. Ilyin, "Gaussian Lattice Boltzmann method and its applications to rarefied flows," *Phys. Fluids* **32**(1), 012007 (2020).
- ¹³⁷S. Hou, Q. Zou, S. Chen, G. Doolen, and A. C. Cogley, "Simulation of cavity flow by the lattice Boltzmann method," *J. Comput. Phys.* **118**(2), 329–347 (1995).
- ¹³⁸T. A. Ho, D. V. Papavassiliou, L. L. Lee, and A. Striolo, "Liquid water can slip on a hydrophilic surface," *Proc. Natl. Acad. Sci. U. S. A.* **108**(39), 16170–16175 (2011).
- ¹³⁹G. H. Tang, W. Q. Tao, and Y. L. He, "Lattice Boltzmann method for simulating gas flow in microchannels," *Int. J. Mod. Phys. C* **15**(02), 335–347 (2004).
- ¹⁴⁰S. Ansumali and I. V. Karlin, "Kinetic boundary conditions in the lattice Boltzmann method," *Phys. Rev. E* **66**(2), 026311 (2002).
- ¹⁴¹X. D. Niu, C. Shu, and Y. T. Chew, "A thermal lattice Boltzmann model with diffuse scattering boundary condition for micro thermal flows," *Comput. Fluids* **36**(2), 273–281 (2007).
- ¹⁴²S. Chapman, T. G. Cowling, and D. Burnett, "The mathematical theory of non-uniform gases: An account of the kinetic theory of viscosity, thermal conduction and diffusion," in *Gases* (Cambridge University Press, 1990).
- ¹⁴³S. Succi, O. Filippova, H. Chen, and S. Orszag, "Towards a renormalized lattice Boltzmann equation for fluid turbulence," *J. Stat. Phys.* **107**(1-2), 261–278 (2002).
- ¹⁴⁴G. H. Tang, W. Q. Tao, and Y. L. He, "Lattice Boltzmann method for gaseous microflows using kinetic theory boundary conditions," *Phys. Fluids* **17**(5), 058101 (2005).
- ¹⁴⁵J. Ren, Q. Zheng, and Y. Li, "Curved boundary condition for lattice Boltzmann modeling of binary gaseous micro-scale flows in the slip regime," *Physica A* **550**, 124181 (2020).
- ¹⁴⁶G. Silva, "Consistent lattice Boltzmann modeling of low-speed isothermal flows at finite Knudsen numbers in slip-flow regime. II. Application to curved boundaries," *Phys. Rev. E* **98**(2), 023302 (2018).
- ¹⁴⁷Y. Peng and L.-S. Luo, "A comparative study of immersed-boundary and interpolated bounce-back methods in LBE," *Prog. Comput. Fluid Dyn., Int. J.* **8**(1-4), 156–167 (2008).
- ¹⁴⁸S. Tao and Z. Guo, "Boundary condition for lattice Boltzmann modeling of microscale gas flows with curved walls in the slip regime," *Phys. Rev. E* **91**(4), 043305 (2015).
- ¹⁴⁹I. Ginzburg and D. d'Humieres, "Multireflection boundary conditions for lattice Boltzmann models," *Phys. Rev. E* **68**(6), 066614 (2003).
- ¹⁵⁰L. Szalmás, "Slip on curved boundaries in the lattice Boltzmann model," *Int. J. Mod. Phys. C* **18**(01), 15–24 (2007).
- ¹⁵¹K. Wang, L. Yang, Y. Yu, and G. Hou, "Influence of slip boundary on the hydrofoil with a curved slip boundary condition for the lattice Boltzmann method," *Phys. Fluids* **30**(12), 123601 (2018).

- ¹⁵²Z. Liu, Z. Mu, and H. Wu, "A new curved boundary treatment for LBM modeling of thermal gaseous microflow in the slip regime," *Microfluid. Nanofluid.* **23**(2), 27 (2019).
- ¹⁵³M. H. Flamm, S. L. Diamond, and T. Sinno, "Lattice kinetic Monte Carlo simulations of convective-diffusive systems," *J. Chem. Phys.* **130**(9), 094904 (2009).
- ¹⁵⁴M. Stamatakis, "Kinetic modelling of heterogeneous catalytic systems," *J. Phys.: Condens. Matter* **27**(1), 013001 (2015).
- ¹⁵⁵J. P. Balbuena and I. Martin-Bragado, "Lattice kinetic Monte Carlo simulation of epitaxial growth of silicon thin films in H₂/SiH₄ chemical vapor deposition systems," *Thin Solid Films* **634**, 121–133 (2017).
- ¹⁵⁶X. Z. An, Y. Zhang, G. Q. Liu, X. G. Qin, F. Z. Wang, and S. X. Liu, "Atomic-scale kinetic Monte Carlo simulation of {100}-oriented diamond film growth in C–H and C–H–Cl systems by chemical vapour deposition," *Chin. Phys. Lett.* **19**(7), 1019–1020 (2002).
- ¹⁵⁷C. C. Battaile and D. J. Srolovitz, "Kinetic Monte Carlo simulation of chemical vapor deposition," *Annu. Rev. Mater. Res.* **32**, 297–319 (2002).
- ¹⁵⁸P. Kratzer, *Multiscale Simulation Methods in Molecular Sciences Lecture Notes* (Institute for Advanced Simulation Jülich Supercomputing Centre, 2009), p. 51.
- ¹⁵⁹M. T. Darby, S. Piccinin, and M. Stamatakis, in *Physics of Surface, Interface and Cluster Catalysis* (IOP Publishing, Bristol, UK, 2016), pp. 4–38.
- ¹⁶⁰M. Stamatakis and D. G. Vlachos, "Unraveling the complexity of catalytic reactions via kinetic Monte Carlo simulation: Current status and frontiers," *ACS Catal.* **2**(12), 2648–2663 (2012).
- ¹⁶¹M. T. Darby, R. Réocreux, E. C. H. Sykes, A. Michaelides, and M. Stamatakis, "Elucidating the stability and reactivity of surface intermediates on single-atom alloy catalysts," *ACS Catal.* **8**(6), 5038–5050 (2018).
- ¹⁶²K. G. Papanikolaou, M. T. Darby, and M. Stamatakis, "Engineering the surface architecture of highly dilute alloys: An ab initio Monte Carlo approach," *ACS Catal.* **10**(2), 1224–1236 (2020).
- ¹⁶³M. E. Naraghi and F. Javadpour, "A stochastic permeability model for the shale-gas systems," *Int. J. Coal Geol.* **140**, 111–124 (2015).
- ¹⁶⁴S. Kirkpatrick, "Percolation and conduction," *Rev. Mod. Phys.* **45**(4), 574–588 (1973).
- ¹⁶⁵M. R. Bonilla and S. K. Bhatia, "Multicomponent effective medium-correlated random walk theory for the diffusion of fluid mixtures through porous media," *Langmuir* **28**(1), 517–533 (2012).
- ¹⁶⁶M. R. Bonilla, R. Valiullin, J. Kärger, and S. K. Bhatia, "Understanding adsorption and transport of light gases in hierarchical materials using molecular simulation and effective medium theory," *J. Phys. Chem. C* **118**(26), 14355–14370 (2014).
- ¹⁶⁷D. A. G. Bruggeman, "Calculation of various physics constants in heterogeneous substances. I. Dielectricity constants and conductivity of mixed bodies from isotropic substances," *Ann. Phys.* **24**(7), 636–664 (1935).
- ¹⁶⁸S. Peng and B. Loucks, "Permeability measurements in mudrocks using gas-expansion methods on plug and crushed-rock samples," *Mar. Petrol. Geol.* **73**, 299–310 (2016).
- ¹⁶⁹A. Tinni, E. Fathi, R. Agarwal, C. H. Sondergeld, I. Y. Akkutlu, and C. S. Rai, *Shale Permeability Measurements on Plugs and Crushed Samples* (Society of Petroleum Engineers, 2012).
- ¹⁷⁰R. N. Moghaddam and M. Jamiolahmady, "Fluid transport in shale gas reservoirs: Simultaneous effects of stress and slippage on matrix permeability," *Int. J. Coal Geol.* **163**, 87–99 (2016).
- ¹⁷¹M. Apostolopoulou, M. Stamatakis, A. Striolo, R. Dusterhoft, R. Hull, and R. Day, "A novel modeling approach to stochastically evaluate the impact of pore network geometry, chemistry and topology on fluid transport," *Transp. Porous Media* (unpublished) (2020).
- ¹⁷²A. Botan, F. J. Ulm, R. J. M. Pellenq, and B. Coasne, "Bottom-up model of adsorption and transport in multiscale porous media," *Phys. Rev. E* **91**(3), 032133 (2015).
- ¹⁷³P. Tahmasebi, F. Javadpour, M. Sahimi, and M. Piri, "Multiscale study for stochastic characterization of shale samples," *Adv. Water Resour.* **89**, 91–103 (2016).
- ¹⁷⁴P. Tahmasebi, F. Javadpour, and M. Sahimi, "Stochastic shale permeability matching: Three-dimensional characterization and modeling," *Int. J. Coal Geol.* **165**, 231–242 (2016).
- ¹⁷⁵U. Tallarek, D. Hlushkou, J. Rybka, and A. Höltzel, "Multiscale simulation of diffusion in porous media: From interfacial dynamics to hierarchical porosity," *J. Phys. Chem. C* **123**(24), 15099–15112 (2019).
- ¹⁷⁶J. Salles, J. F. Thovert, R. Delannay, L. Prevors, J. L. Auriault, and P. M. Adler, "Taylor dispersion in porous media. Determination of the dispersion tensor," *Phys. Fluids A* **5**(10), 2348–2376 (1993).
- ¹⁷⁷D. Hlushkou, A. Svidrytski, and U. Tallarek, "Tracer-size-dependent pore space accessibility and long-time diffusion coefficient in amorphous, mesoporous silica," *J. Phys. Chem. C* **121**(15), 8416–8426 (2017).
- ¹⁷⁸R. Erban, "From molecular dynamics to Brownian dynamics," *Proc. R. Soc. London, Ser. A* **470**(2167), 20140036 (2014).
- ¹⁷⁹J. R. Kalnin, E. A. Kotomin, and J. Maier, "Calculations of the effective diffusion coefficient for inhomogeneous media," *J. Phys. Chem. Solids* **63**(3), 449–456 (2002).
- ¹⁸⁰J. K. Holt, H. G. Park, Y. M. Wang, M. Stadermann, A. B. Artyukhin, C. P. Grigoropoulos, A. Noy, and O. Bakajin, "Fast mass transport through sub-2-nanometer carbon nanotubes," *Science* **312**(5776), 1034–1037 (2006).
- ¹⁸¹S. Kim, F. Fornasiero, H. G. Park, J. B. In, E. Meshot, G. Giraldo, M. Stadermann, M. Fireman, J. Shan, C. P. Grigoropoulos, O. Bakajin, "Fabrication of flexible, aligned carbon nanotube/polymer composite membranes by in-situ polymerization," *J. Membr. Sci.* **460**, 91–98 (2014).
- ¹⁸²N. Bui, E. R. Meshot, S. Kim, J. Peña, P. W. Gibson, K. J. Wu, and F. Fornasiero, "Ultradurable and protective membranes with sub-5 nm carbon nanotube pores," *Adv. Mater.* **28**(28), 5871–+ (2016).
- ¹⁸³Y. Baek, C. Kim, D. K. Seo, T. Kim, J. S. Lee, Y. H. Kim, K. H. Ahn, S. S. Bae, S. C. Lee, J. Lim, K. Lee, and J. Yoon, "High performance and antifouling vertically aligned carbon nanotube membrane for water purification," *J. Membr. Sci.* **460**, 171–177 (2014).
- ¹⁸⁴F. Du, L. Qu, Z. Xia, L. Feng, and L. Dai, "Membranes of vertically aligned superlong carbon nanotubes," *Langmuir* **27**(13), 8437–8443 (2011).